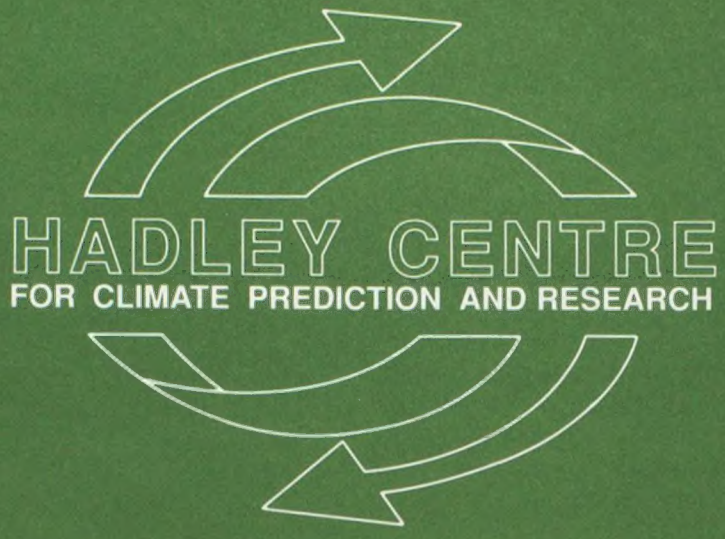

A comparison of modelled surface fluxes with climatological estimates

by

C Gordon and D K Wright

CRTN 53

March 1995

CLIMATE
RESEARCH
TECHNICAL
NOTE

Hadley Centre
Meteorological Office
London Road
Bracknell
Berkshire RG12 2SY

CLIMATE RESEARCH TECHNICAL NOTE NO. 53

A COMPARISON OF MODELLED SURFACE FLUXES WITH CLIMATOLOGICAL ESTIMATES

by

C Gordon and D K Wright

Hadley Centre for Climate Prediction and Research
Meteorological Office
London Road
Bracknell
Berkshire RG12 2SY

NOTE: This paper has not been published. Permission to quote from it should be obtained from the Director of the Hadley Centre.

INTRODUCTION

The purpose of this report is to compare the ocean surface fluxes, as simulated by the Hadley Centre atmospheric model running in climate mode, with climatological estimates of these fluxes derived from ship observations and cloud climatologies. It is well known that these flux climatologies have large uncertainties, both because of the flux parametrizations and, in many areas over the world oceans, because of lack of relevant data. The purpose of this report is therefore not so much to attempt to validate the model fluxes in an absolute sense, for this is not possible, but rather to determine those regions where the model values lie outside the error bounds on the climatological estimates and therefore indicate systematic inadequacies in the model simulation. It should, of course, also be born in mind that the comparisons described here refer to one particular version of the model and that the model itself is continually being upgraded.

The differences between the model and climatology are also compared with the flux correction fields that are diagnosed when the atmosphere is coupled to a global ocean model. This comparison enables us to establish, to some degree, just how much of the 'flux correction' can be attributed to shortcomings in the atmospheric model fluxes and how much to inadequacies in the ocean model simulation.

BACKGROUND

This report will compare a climatology of surface fluxes extracted from the Hadley Centre climate version of the Unified Model with the heat flux climatology of Oberhuber (1988) and the wind stress climatology compiled by Hellerman and Rosenstein (1983). These climatologies have inherent uncertainties associated both with sparsity of data and with the bulk formulations used to derive the fluxes.

The data used in preparation of the Oberhuber compilation was based on the COADS (Comprehensive Ocean Atmosphere Dataset) as described by Woodruff et al. (1987) and prepared by Wright (1988). The surface net solar radiation was calculated from the daily averaged short wave radiation flux at the top of the atmosphere and corrected after Zillman (1972) for relative humidity and inclination and after Reed (1977) for cloudiness. The net surface long wave radiation was calculated after Berliand (1952) using sea and air temperatures and relative cloud cover. The latent and sensible heat fluxes were calculated via bulk formulae using the transfer coefficients of Large and Pond (1981,1982) with a modification to allow for the increase of the exchange coefficient with wind speed using the Charnock relation.

Kent and Taylor (1995) have compared a number of North Atlantic latent and sensible heat flux climatologies (including Oberhuber) with 'best estimates' obtained using ship data with transfer coefficients from recent air-sea interaction experiments. The results indicate that many of the flux calculations, including Oberhuber, over-estimate the surface turbulent fluxes from the ocean. Oberhuber artificially enhances the heat fluxes by increasing the Charnock constant (see later) in order to obtain reasonable ocean meridional heat transports. Despite its limitations we use Oberhuber in this note as our main climatology with which to compare the model because it has a surface flux

formulation very similar to that used in the atmospheric model and it is nearly global in extent. Comparisons have also been made with the Esbensen and Kushnir (1981) climatology. Overall the identification of the major model flux errors does not depend on the climatology used. The uncertainty in the climatology does, however, mean that over much of the world oceans we cannot verify the model flux simulation.

The Hellerman and Rosenstein (1983) climatology of global wind stresses was based on over 35 million wind observations taken between 1870 and 1976 compiled by the National Climate Centre in Asheville. Due to the nature of shipping lanes, areas both rich and sparse in observations exist. The wind stresses were calculated using the drag coefficients of Bunker (1976). As explained later, these are probably too large in regions of relatively low winds, particularly in the equatorial regions.

These climatologies are prone to many uncertainties. The amount of data available over large areas of the globe is very sparse meaning that there are either no estimates in those areas, or they are prone to large errors. The exact techniques used to calculate the fluxes and stresses are also a topic of debate. Rowntree (unpublished note, 1993) pointed out that Oberhuber's climatology of surface net solar radiation has values which are, possibly, too low in tropical regions. Quinn and Burt (1968) show 12 years of monthly data of annual mean net surface solar flux for Canton Island in the equatorial Pacific which, when compared with Oberhuber's fluxes, suggests an underestimate of over $50Wm^{-2}$ at that location. In middle latitudes, at OWS 'P' in the Pacific and OWS 'I' in the Atlantic, the Oberhuber values compare well with observed radiometer data (Mitchell, 1977). At these locations the Oberhuber fluxes are typically only 5 - $10Wm^{-2}$ less than the observations which is within the overall uncertainties. The Esbensen and Kushnir (1981) solar heating values are typically 20 - $30Wm^{-2}$ larger than the Oberhuber values in the tropics which is a further indication that the Oberhuber values may underestimate this flux. Oberhuber also arbitrarily reduced the solar flux by 10% in order to fit the observed ocean heat transports.

The Hellerman and Rosenstein wind stresses may be too large in many regions (Harrison, 1989). This is due to the way the increase in the drag coefficients with wind speed is treated. Harrison used the same data but (lower) drag coefficients which were based on those of Large and Pond (1981). These produced differences in the zonal wind stresses between the two datasets of 25% to 30% in the annual mean of the trade winds and 20% to 30% in the region of maximum northern hemisphere westerlies. In all cases the Hellerman and Rosenstein stresses were larger than those calculated by Harrison. However, it is thought that the Hellerman and Rosenstein wind stresses in the southern ocean may be too weak.

Despite the uncertainties, these climatologies are still useful for comparisons of model runs with observed climate, as long as these factors are born in mind. These climatologies cannot realistically be used as definitive estimates of the different fluxes but they can be used to establish whether the models produce fluxes that are within the uncertainty of the climatologies based on observations. (The precise uncertainty in the climatological estimates is not known and is dependent upon the bulk formulae, data coverage etc. However, comparison with different climatological estimates does give some indication as to the uncertainty. A definitive statement of the uncertainty in the climatological estimates, taking into account all factors, would be very useful). Fluxes

derived operationally from Numerical Weather Prediction (NWP) models are another source of data for comparison but the model flux differences in these NWP data sets are also very large (Foreman et al, 1994).

In the version of the Hadley Centre climate model from which the fluxes used in this investigation were taken, the atmospheric model is coupled to a fully interactive dynamic ocean model. Both models have the same horizontal grid and a strong linear relaxation to climatology is used to restrain the SST field to remain close to its climatological values. The model therefore effectively has climatological SSTs. The purpose of the particular simulation studied was to define the flux corrections terms for use in subsequent climate change experiments and it was used in place of a straight atmospheric only model integration to allow direct comparison of the simulated fluxes and flux corrections.

The atmospheric model is formulated on a 2.5°x3.75° latitude-longitude grid with 19 levels in the vertical. It is a version of the Meteorological Office Unified Model used for both operational weather forecasting and climate research (Cullen, 1991). It contains detailed physical parametrizations including the use of an interactive cloud scheme. The coupled model version used here was also used for the latest series of climate change coupled experiments carried out at the Hadley Centre (Hadley Centre, 1995). The coupled model was integrated for a period of 55 years (including a 40 year ocean only spin-up) and the diagnostic output was meaned over the last 5 years of the run to produce the model flux climatology used in this note.

TURBULENT FLUX FORMULATIONS

As the surface turbulent fluxes are dependent upon the flux formulation used, both in the model and the climatologies, it is worth comparing the different schemes. A similarity method is used to calculate the surface exchange coefficients in both the model and Oberhuber. The actual coefficient depends upon the reference level. In order to compare the two schemes we express the implied model neutral values for the heat and moisture exchange coefficients as (Smith, 1993):

$$C_H(z) = C_L(z) = (k / \ln(z / 10^{-4}))x(k / \ln(z / z_0))$$

where z is the reference level height, z_0 is the roughness length for momentum and k is the von Karman constant, taken in the model and Oberhuber to be 0.4. C_H and C_L are the neutral exchange coefficients for sensible and latent heat respectively. The surface roughness length in the model is calculated as:

$$z_0 = \max(10^{-4}, c_{char} u_*^2 / g)$$

where u_* is the friction velocity, g the gravitational acceleration and C_{char} is the Charnock coefficient. For a reference level of 10m this gives:

$$C_H(10) = C_L(10) = 0.0347(k / \ln(10 / z_0))$$

when the model value C_{char}=0.012 for the Charnock coefficient is used.

In calculating the fluxes from observed data, Oberhuber (1988, equations 16 and 17) uses the same theory with:

$$C_H = 0.0327k / \ln(10 / z_0)$$

$$C_L = 0.0346k / \ln(10 / z_0)$$

and C_{char}=0.032. This high value of the Charnock coefficient was used by Oberhuber to fit the calculated heat fluxes to the observed northwards oceanic heat transports. Oberhuber does not specify a minimum value of z_0 as calculated from the Charnock formula. Taking C_D=1.4x10^{-3} in the calculation of u* and a reference level of 10m, the following table compares the neutral values of C_L and C_H for different wind speeds:

Wind Speed (ms^{-1})	z_0^{Mod} (x10^4)	z_0^{Ober} (x10^4)	$C_L^M(=C_H^M)$ (x10^3)	C_L^O (x10^3)	C_H^O (x10^3)	C_L^M/C_L^O	C_H^M/C_H^O
4	1.00	0.73	1.21	1.17	1.11	1.03	1.09
6	1.00	1.64	1.21	1.26	1.19	0.96	1.02
10	1.71	4.57	1.26	1.39	1.31	0.91	0.96
14	3.36	8.95	1.35	1.49	1.41	0.91	0.96

Comparison of the Model and Oberhuber roughness lengths and exchange coefficients for various wind speeds

For moderate and high wind speeds the model neutral exchange coefficients are lower than those used by Oberhuber. The main reason for the larger Oberhuber coefficients is the larger value of the Charnock coefficient used by Oberhuber to fit the ocean heat transports. We can conclude that, at least in neutral conditions (see the section on latent heat fluxes for a comparison in unstable conditions), that the bulk parametrizations are not too dissimilar in the model and Oberhuber but that in the model values of the sensible and latent heat fluxes can be expected to be slightly lower than those of Oberhuber.

COMPARISON OF FLUXES

In order to make a comparison of the model climatology of fluxes with the observed estimates the two seasons corresponding to the months of December-January-February ('Winter') and June-July-August ('Summer') are looked at in detail. Each of the momentum and heat flux components are analysed in turn and, at the end, the total net surface heating is compared.

For the wind stresses three figures are shown which are the modelled and climatological stresses in each season and the differences in the magnitude of the stresses. For the heat fluxes three figures are also shown in each case - the model, Oberhuber and the model minus Oberhuber difference fields. Where appropriate, comparisons are also made with the Esbensen and Kushnir climatology and satellite radiation data.

Surface Wind Stress

June-July-August. Figs.1a and 1b show the modelled and climatological summer season wind stresses from the model and Hellerman and Rosenstein and fig.1c shows the difference in magnitudes. The overall magnitudes of the stresses from the model compare well with climatology, although there are specific regions where the deviation from Hellerman and Rosenstein is probably greater than the uncertainty in the climatological estimates. In these regions the differences can usually be associated with known systematic errors in the model simulation. Looking at the magnitude of the wind stress, the model wind stresses are too strong in middle to high latitudes of the Southern Hemisphere. Hellerman and Rosenstein are thought to be too weak in the Southern Ocean, and this possibly accounts for some of this difference, but it is also known that the model sea level pressure gradient is too strong between the Antarctic low pressure system and the southern hemisphere sub-tropical highs and this is likely to be the main cause of these large differences.

The strong surface stresses associated with the trade winds in both hemispheres are slightly underestimated compared to Hellerman and Rosenstein. It has been suggested that the Hellerman and Rosenstein drag coefficients are too high in these regions and the recalculation by Harrison (1989) led to stresses that were 20 - 30% lower than Hellerman and Rosenstein. The model stresses in the sub-tropics lie between these two and compared to the estimates of Harrison (1989) they are slightly too large. This is consistent with an over-intense Hadley circulation in the model when compared to various estimates from observations and numerical model analyses.

The model Indian monsoon winds extend too far east, into the west Pacific, and this is a known characteristic of the monsoon simulation in the atmospheric model.

The stresses in the far east Pacific are particularly important because of their direct impact on SST through coastal upwelling. In coupled experiments with GCMs the proper simulation of the cold SSTs associated with this upwelling (and also with the presence of marine stratocumulus in the region, reducing sunlight) has been a particular problem. Figs.1d and 1e show the September wind stress from the model

and Hellerman and Rosenstein for the east Pacific region. September is chosen as this is the time of year when the coastal upwelling is near a maximum. In the climatology stresses in excess of 0.5 dyne/cm^2 are present along the South American coastline. In the model, however, the stresses are considerably weaker along this coastal region and their direction is not consistently northerly. The reason for this may well be related to inadequate representation of the very steep topography associated with the Andes.

December-January-February. Figs.2a and 2b show the modelled and climatological winter wind stresses and fig.2c shows the difference in wind stress magnitudes. In the model simulation the peak stresses over the North Atlantic are smaller in the model than in the Hellerman or the Harrison datasets. This suggests that the modelled surface winds may be too light in these regions and this needs further investigation.

The stresses in the north west Pacific (near Kamchatka) are north-easterly instead of north-westerly and the maximum is shifted to the east so that there is a large westerly component of the stress across the width of the Pacific. These differences in the north Pacific between the model and climatology are due to the low pressure region in the model being, generally, too far to the east. It is also too deep with a low of around 992mb compared with around 1000mb in the analysis.

The trades are generally slightly lower in strength than those in the Hellerman and Rosenstein climatology but are larger than the Harrison climatology (not shown), making the trade stresses slightly too large but still within the uncertainty in the climatological estimates. A particularly significant difference, in relation to the use of the model in El Nino prediction experiments, is the short extension of the model SE trades into the central Pacific. This makes the model stresses very weak in this region and this will have a significant effect on the equatorial thermocline in the ocean. It also affects the local evaporation in these regions.

In Hellerman and Rosenstein and the model there is a relatively strong seasonal signal in the easterly stresses to the east of Australia. In the model this would appear to be over emphasised (again keeping in mind that Hellerman and Rosenstein is too large anyway) with the DJF stresses rising to over 0.1 N/m^2 in this region. As will be seen later these large winds have a significant effect upon the latent heat flux there.

The stress associated with the Southern Hemisphere westerlies is also too large at this time of year.

Surface Net Short Wave Radiation.

June-July-August. Figs.3a, b, c show the net surface short-wave radiation from the model, Oberhuber and the difference between the model and Oberhuber. Note the lack of data in the Southern Hemisphere in Oberhuber. The difference chart (fig.3c) indicates that the model tropical and sub-tropical values are 25 - 50Wm^{-2} higher than Oberhuber in most areas. This difference has been discussed in the introduction. The exception is the North Pacific and North Atlantic where the net short wave heating is underestimated compared to Oberhuber. This suggests that the model has excessive cloud over the northern hemisphere oceans in summer. This is confirmed by

comparison of the planetary albedo from the model and from the ERBE (Earth Radiation Budget Experiment) data (see fig.4 for which ERBE data from 1985-87 were used). The figure shows the model albedo is too high in summer in the northern ocean regions, consistent with an excessive cloud amount.

In the marine stratocumulus areas off the west coast of South America the model values are considerably larger than those of Oberhuber. Comparison with ERBE data (fig.4) shows the modelled planetary albedo in this area is too low, associated with the underestimation of low cloud by the model in this region. This is a well known systematic error of the model and attempts are currently in progress to improve the stratocumulus simulation. This error has particular impact in coupled ENSO simulations where the lack of stratocumulus leads to permanent El Nino-type conditions in the eastern tropical Pacific. A similar error is evident off the African coast in the south east Atlantic. This is also confirmed by the ERBE data which again points to there being too little cloud in this region.

The Esbensen and Kushnir fields of short wave heating, although larger in overall magnitude, especially in the tropics, have much the same pattern as Oberhuber. As discussed in the introduction the Oberhuber tropical values may well be too low.

December-January-February. The winter-time modelled, climatological and difference fields are shown in figs.5a, b, c. Once again the model values are generally 25 - 50Wm^{-2} higher in the model than in Oberhuber's climatology in almost all tropical areas. The differences in the coastal stratocumulus areas persist into this season.

In the region to the south-east of the South Pacific Convergence Zone (SPCZ) (around 135°W) the model has similar values to Oberhuber. In reality, this indicates another well known systematic error in the model, which is the tendency for the SPCZ in terms of rainfall and cloudiness to extend too far into the east Pacific leading to an underestimation of the short wave flux reaching the surface. This is illustrated by the summertime precipitation fields shown in figs.5d and 5e. The climatological field is from the dataset of Legates and Willmott (1990). The model over-extension of the SPCZ out into the east Pacific is apparent in the rainfall fields from the model and this can also be seen in the comparison of model planetary albedo with that from ERBE (fig.4b).

Surface Net Long Wave radiation

June-July-August. The surface net long wave flux from the model, Oberhuber and differences are shown in figs.6a, b, c. The model and Oberhuber values compare well in terms of the overall magnitude and the pattern of the fields. The marine stratocumulus cloud errors referred to in the discussion of the short wave flux are also evident in the long-wave heating. Over most of the oceans the differences are within the range ±20Wm^{-2}.

December-January-February. The winter-time fields are shown in figs.7a,b and c. The general pattern shows a close similarity to Oberhuber. Some of the largest differences occur in the northern tropical Atlantic off the coast of Africa which is

presumably related to the underestimation of cloud in this region. Once again, across most of the ocean, the differences are within the uncertainty in the data.

Latent Heat

June-July-August. The summer-time latent heat fields are shown in figs.8a, b and c. It is clear that the model values are generally larger in the tropics and sub-tropics by up to $50Wm^{-2}$ though over most of the oceans the model and Oberhuber values agree to within $25Wm^{-2}$. This is a consistent feature across all oceans. As noted above, the trade stresses in the model are probably too large and this could account for some of the increased evaporation. There are also large differences in the monsoon regions which are also presumably related to the difference in surface winds. The large differences to the east of Australia may well, in part, be associated with the relatively high modelled winds in this region compared to climatology. There is also considerably more evaporation in the model than in Oberhuber to the north and west of Australia.

Another important difference between the model and Oberhuber formulations of the exchange coefficients is the dependence on the boundary layer stability. It was shown earlier that the neutral Oberhuber values of C_E are larger than those in the model. In addition, in the model scheme, specific account is taken of the low wind unstable scenario, the so called 'free convective limit'. This was included because past experience had shown the model to be sensitive to the parametrization of evaporation in these low wind unstable conditions (Gordon, 1988; Miller et al,1992). Details of the model scheme can be found in Smith (1993).

Fig.10 shows plots of the latent heat exchange coefficient, for various wind speeds, and as a function of the bulk Richardson number Ri_b (see the Appendix for a detailed explanation of the exchange coefficient formulation in terms of Ri_b). In unstable conditions, especially at low wind speeds, the model coefficients are considerably larger than those calculated using Oberhuber's scheme. The different coefficients could account for some of the tropical differences in the latent heat flux fields in figs.8 and 9.

December-January-February. The winter latent heat fields in figs.9a, b and c also show a broad scale similarity between the model and Oberhuber. As in the summer, over most of the oceans the model and Oberhuber values again agree to within $25Wm^{-2}$. The model shows comparable evaporation to Oberhuber over the relatively warm waters of the Gulf Stream and Kuroshio. As in the summer over much of the tropical and sub-tropical oceans there is greater model evaporation than in Oberhuber (or Esbensen and Kushnir) with particularly large differences under the Pacific north-east trades, in the Arabian Sea and Bay of Bengal and the strong winds to the east of Australia (see fig.2). An exception is the equatorial region just east of the dateline where there is less evaporation in the model than Oberhuber. This corresponds to the region in winter where the SE trades are very weak in the model as discussed earlier.

Sensible Heat Flux

June-July-August. The summer-time sensible heat fluxes are shown in figs.11a, b and c. The model has larger fluxes in the tropics (10 to 20 Wm^{-2} upward flux) compared with Oberhuber (between 0 and $10Wm^{-2}$). As the heat exchange coefficient is very similar in Oberhuber and the model the too large flux suggests the model is maintaining too high a temperature difference at the ocean atmosphere interface. This is confirmed by comparison of the model air-sea temperature differences with data from ocean weather ships (Hall, unpublished note) which shows that in all areas looked at the model overestimates this difference. This excessive air-sea temperature difference will also contribute to the large latent heat fluxes in the model. In the tropical regions the model sensible heat exchange coefficient will also be larger than that used by Oberhuber for the reasons discussed in the previous section.

December-January-February. The winter-time sensible heat fluxes are shown in figs.12a, b and c. The general pattern in the model is quite similar to Oberhuber with the flux in most places having values less than $20Wm^{-2}$. In the regions of the Gulf Stream and Kuroshio there are considerably larger differences with the Pacific maxima around $140Wm^{-2}$ for the model and $100Wm^{-2}$ for Oberhuber. The north Atlantic maxima are more similar being about $100Wm^{-2}$ in both cases.

The Total Surface Heat Flux

June-July-August The total surface heat flux for summer is shown in figs.13a, b and c. The difference chart between the model and Oberhuber highlights a number of regions that show particularly significant differences. In the North Pacific region the model has considerably less heat entering the ocean than indicated by the Oberhuber climatology. Reference to the individual component difference maps shows that this predominently arises from the lower surface short wave fluxes in the model compared to Oberhuber.

The difference chart fig.13c also indicates that the region in the South Pacific to the east of Australia has less heat entering the ocean than implied by the Oberhuber climatology. Again referring to the individual heat flux components it can be seen that in this region the difference arises because of the greater latent heat losses in the model compared to Oberhuber, so that the total heat flux difference pattern in this region reflects the latent heat difference pattern. There are also large differences in the Indian Ocean net heat flux and these also appear to arise from the latent heat flux differences. The reasons for the differences in latent heat flux have already been discussed above.

For comparison fig.15a shows the difference in the net surface heating between the Oberhuber and Esbensen and Kushnir climatologies. This difference gives some indication as to the uncertainty in the climatological fluxes. In general there is closer agreement between the two climatologies than between either climatology and the model which indicates these climatologies are still useful in verifying the model fields. It is interesting that in the North Pacific region the Esbensen and Kushnir dataset suggests a net surface heat loss of $40Wm^{-2}$ less than Oberhuber and is therefore more

in agreement with the model. As already discussed, however, the ERBE albedo measurements suggest that the model does overestimate the cloud in this region.

December-January-February The winter-time net surface heating (figs.14a & b) shows large heat losses over the warm waters of the Gulf Stream and the Kuroshio. The major differences in this total flux (fig.14c) occur in these regions, underneath the NE trades and in the South Pacific to the east of Australia as discussed for the summer fields. There are also significant differences in the Indian Ocean. Comparison of the latent heat flux differences (fig.9c) with this net winter heating difference shows that the latter is dominated by the latent heat flux differences. Once again, the indication is that there is considerably greater evaporation in the model than implied by the Oberhuber data.

For comparison fig.15b shows the net heat flux difference between the climatological estimates of Oberhuber and Esbensen and Kushnir. The largest differences are in the region of the western boundary currents - as might be expected - but overall the climatologies are still closer to each other than either is to the model fields.

The major differences between the component heat fluxes from the model and the climatologies are summarised in Table 1.

FLUX ERRORS AND FLUX CORRECTIONS

When coupled ocean-atmosphere models of the climate system are integrated over extended periods of time, it is often the case that the simulated climate drifts away from that observed to such an extent that the basic model state is not a suitable control around which to investigate climate perturbations. This is the problem of climate drift.

In order to reduce the systematic errors and keep the model climate closer to reality, artificial forcing terms are often added to the fluxes simulated at the ocean-atmosphere interface. The use of this flux correction technique compensates for a wide variety of different errors in both the atmosphere and ocean models (Sausen et al, 1988). Clearly, the comparison of model simulated fluxes with climatological estimates can go some way to establishing the contribution to the flux correction that arises from systematic errors in the GCM fluxes, rather than, for example, from errors inherent in the ocean model simulation (see later). In this section flux corrections from the coupled model will be compared with the flux differences already discussed. As already mentioned, the ocean component of this coupled model consists of a global ocean model on the same 2.5°x3.75° latitude-longitude grid as the atmospheric model. The exact details are not important to the discussion that is to follow.

The method used to define the flux correction in the simulation described here is that of Murphy (1995) and Manabe et al (1991). As the coupled model is integrated a correction term is added to the surface fluxes to ensure that the SSTs and the surface

correction term is added to the surface fluxes to ensure that the SSTs and the surface salinities remain close to their seasonally varying climatological values. For example, the air-sea heat flux (Q) is given by:

$$Q(T) = Q_M + \lambda(T_C - T)$$

where Q_M is the air-sea flux calculated by the atmospheric model, T_C is the seasonally varying climatological SST, T the SST predicted in the ocean model and λ the relaxation coefficient. This is equivalent to the simple linear feedback forcing introduced into ocean modelling by Haney (1971). The consequent forcing terms λ (Tc-T) were averaged over the last few years of the integration. A value of λ ($=163 Wm^{-2}K^{-1}$) considerably larger than the 'physical' values suggested by the calculations of Haney (1971), and subsequent calculations, were used in the application of the correction procedure for the run considered here. In the context of flux correction the value of λ is chosen so as to ensure the predicted SSTs remain 'close' to climatology, where the relaxation coefficient λ determines how close. Once stable flux corrections have been determined, the coupled model is integrated with these corrections applied as seasonally varying constant increments.

The heat flux corrections when calculated as described above are, in certain areas, of a similar size to the air-sea flux itself. Since these flux correction terms have no physical basis, it is clearly necessary to try and reduce their size and eventually the need for them altogether by improving the ocean and atmosphere models. Comparison of the flux correction fields with the flux differences already discussed gives some indication as to the source of the errors.

If in the coupled model the ocean component were 'perfect' in the sense that if it were given the correct forcing it would reproduce the observed seasonal cycle of SST then all of the flux correction could be attributed to atmospheric flux errors. In practice the ocean models in current use are far from perfect and the flux correction is also compensating for inadequacies in the ocean component. However, it is still worth comparing the flux differences discussed in this note with the flux corrections because if there are similarities in the fields it does provide further evidence of (although not definitively) problems with the model heat fluxes.

Before looking at the flux correction fields it is worth considering what systematic errors we might expect from the ocean models that will contribute significantly to the flux correction. One major error is the representation of the narrow ocean currents such as the Gulf Stream and the Kuroshio. The ocean models cannot properly represent these currents with the coarse resolution grids that are used and, inevitably, large flux corrections occur in these regions. Other regions that are particularly difficult to represent in the model are the narrow equatorial and coastal upwelling regions and once again large flux corrections can be expected in these regions arising from systematic errors in the ocean model simulation.

Figs.16a and b show the summer and winter flux correction fields from the same period in the coupled integration as the surface flux fields shown earlier. These fields

will be compared with the model minus Oberhuber total heat flux differences shown in figs.13c and 14c.

Many of the regions of large implied flux corrections are associated with regions of high horizontal gradients of SST, since the coupled model does not correctly position (or even represent) these high gradient regions. It is inevitable that in a region of high SST gradient, even a small shift in the modelled SST pattern away from the climatological pattern will lead to large flux corrections. Indeed, it raises questions as to whether these regions should be corrected at all. A full discussion of these issues can be found in Roberts and Gordon (1995). In what follows the main interest is in open ocean regions away from these gradients. In these regions the local surface heating plays a dominant role in determining the SST.

Comparison of the summer model minus Oberhuber difference field in figs 13c with the flux correction field in fig.16a reveals a number of similarities. In the North Pacific both indicate there is too little heat entering the ocean. The peak in the flux correction in the western North Pacific is probably associated with the positioning of the SST distribution associated with the Kuroshio current. The peak in the north west is likely to be associated with the excessive cloud in these region as discussed in the section on shortwave heating. The model minus ERBE albedo difference in fig.4 also confirms this. The stratocumulus region in the east Pacific is also evident in both plots emphasising the lack of marine stratocumulus cloud in the model simulation.

Large differences also occur to the east of Australia stretching out across the Pacific. In both the flux difference and the flux correction these indicate too little heating of the ocean. By comparison with the results for the individual differences these are most likely dominated by the large latent heat fluxes in the model in this region which have already been discussed. Other marked similarities in pattern exist in the Indian Ocean, immediately west of Australia, and in the Arabian Sea and Bay of Biscay. The large flux corrections in the Southern Ocean, evident in fig 16a, do not show up in the data sparse areas in the flux difference in fig.13c. However, it is likely that many of these peaks in the flux correction arise from a displacement of the high SST gradients associated with the Antarctic Circumpolar Current and they should not be wholly associated with surface flux errors.

The winter flux differences are shown in fig.14c and the flux corrections in fig.16b. The flux correction field indicates too much heating in the north east Pacific region at this time of year, although there is no evidence of this in the flux difference or the albedo differences. At this time of year there are large differences associated with the Gulf Stream and the Kuroshio. These arise because in winter there is cold air moving over a warmer sea and very large latent heat losses ensue. How much the large flux corrections in these regions arise from systematic errors in the atmospheric model flux calculations and how much from the misrepresentation of the Gulf Stream and the Kuroshio in the ocean model is difficult to determine.

Both the flux difference and correction indicate there is too much heating of the ocean in the central equatorial Pacific. Comparison with the component fields indicates that this arises from too little evaporation in this region associated with the low winds simulated in the model (see section on wind stress and latent heat flux). The excessive

cooling of the ocean to the east of Australia, present in the summer, also persists into the winter. The flux correction indicates too strong heating off the coast of Africa in the tropical Atlantic. The model minus ERBE albedo difference in fig.4b suggests that this is associated with an underestimation of the cloud in this region although the representation of coastal upwelling in the ocean model will also be important here. Once again nothing definitive can be said about the differences in the Southern Ocean.

The above results are summarised in Table 2. The table indicates those parts of the flux correction field that are likely to be due to flux errors and the possible causes of these errors. As the climatological flux data are poor this table should only be taken as indicative of regions worth further investigation.

SUMMARY

This note has compared the surface flux fields from an atmospheric GCM simulation with estimates of these fields from climatology. Although there are large uncertainties in the climatologies, in some regions the model errors lie outside the range of these. This give some indication of the areas to focus on in terms of the model developments required to improve the surface fluxes. In addition, these flux differences have been compared with the flux corrections derived when the atmospheric GCM is coupled to an ocean GCM. In many regions there is a correspondence between the flux correction patterns and those obtained in the total flux difference - another indication of the areas that specifically need improvement.

As the net surface heat flux is not known to within $20Wm^{-2}$ or so, little can be said about the regions where the model fluxes lie within this uncertainty and which comprise the majority of the ocean-covered areas. Better climatological datasets of surface fluxes are needed to validate the flux simulations in coupled models over these areas.

Finally, it is recognised that the results presented in this note are specific to a particular version of the atmospheric GCM used here and that as a consequence of further research and development 'improved' versions are appearing continuously. The results presented in this note, however, should help to focus attention on which regions in the present version of the model need particular attention in the future. Comparison of these results with those produced by other atmospheric GCMs would also be very useful.

ACKNOWLEDGEMENTS

We would like to thank Dr. Tim Johns and his staff who carried out the GCM integration discussed in this paper and made the results readily available.

APPENDIX

THE UNSTABLE EXCHANGE COEFFICIENTS IN TERMS OF THE BULK RICHARDSON NUMBER

The bulk Richardson number Ri_B is defined by:

$$Ri_B = (z + z_0)\Delta B / V^2 \qquad \text{(A1)}$$

where ΔB is the buoyancy difference between the surface and the reference level and V is the reference level wind speed. Ri_B is a measure of stability in the boundary layer and is related to the Monin-Obukhov length L by:

$$z / L = k \frac{C_H}{C_D^{3/2}} Ri_B \,. \qquad \text{(A2)}$$

(See Oberhuber (1988) and Smith (1993) for a further discussion of terms.)

In the atmospheric model the unstable exchange coefficients are calculated as:

$$C_L = C_{LN} f_h \qquad \text{(A3)}$$

$$f_h = 1 - \frac{A_h Ri_B}{(1 + B_h(-Ri_B)^{1/2})} \qquad \text{(A4)}$$

$$B_h = \frac{A_h C_{LN}}{f(z, z_0, z_{0f})} \qquad \text{(A5)}$$

where C_{LN} is the neutral coefficient and z_{0f} is the 'free convective limit roughness length' (Smith, 1993). In the model the empirical constant A_h is set equal to 10 and the free convective roughness length is estimated by scaling arguments. The resulting expression for ' f ' for a 10m reference level is:

$$f = \frac{1}{4}\left(\frac{1.3 \times 10^{-3}}{10 + z_0}\right)^{1/2} \qquad \text{(A6)}$$

Using the above formula the value of C_L can be calculated as a function of Ri_B.

The Oberhuber coefficients use the scheme of Large and Pond (1982) in which the unstable coefficient is calculated as:

$$C_L = \frac{C_{LN}(C_m / C_{mN})^{1/2}}{1 - k^{-1} C_{LN} C_{mN}^{-1/2} \Psi_L} \qquad \text{(A7)}$$

$$(C_m / C_{mN})^{1/2} = \left[1 - C_{mN}^{1/2} k^{-1} \Psi_m\right]^{-1} \qquad \text{(A8)}$$

$$\Psi_L = 2\ln\left[\frac{1+X^2}{2}\right] \qquad \text{(A9)}$$

$$\Psi_m = 2\ln\left[\frac{1+X}{2}\right] + \ln\left[\frac{1+X^2}{2}\right] - 2\arctan X + \pi/2 \qquad \text{(A10)}$$

where X, by using the above relationship (A2) between Ri_B and the Monin-Obukhov length, is given by:

$$X = \left[1 - 16k\frac{C_L}{C_m^{3/2}} Ri_B\right]^{1/4}. \qquad \text{(A11)}$$

In this case C_L is calculated iteratively starting with the neutral coefficients and then iterating the above equations to obtain a convergent value of C_M and C_L for each value of Ri_B.

The unstable coefficients have a wind speed dependence both from the roughness length z_0 and through the bulk Richardson number defined in (A1). In the free convective limit the wind speed V tends to zero and the asymptotic values of the coefficients calculated by the two schemes above are quite different. Fig. 10 shows the latent heat exchange coefficient as a function of Ri_B. Curves are presented for different wind speeds. Note that from the definition of Ri_B in (A1), for a fixed wind speed, increasing (negative) Ri_B implies increasing boundary layer instability (i.e. increasing air-sea temperature difference).

TABLE 1: SUMMARY - SURFACE FLUX DIFFERENCES THE MODEL COMPARED TO CLIMATOLOGY

FLUX	SUMMER	WINTER
Wind Stress	1) Southern Hemisphere westerly stress is too large. 2) Trade stresses in both hemispheres are slightly too large. 3) Surface westerlies associated with the Indian Monsoon extend too far into the west Pacific. 4) East Pacific stresses along the South American coast are too weak.	1) Southern Hemisphere westerly stress is too large. 2) Trade stresses in both hemispheres are slightly too large. 3) The central equatorial Pacific stresses are too weak. 4) N. Atlantic stresses are too weak. 5) N. Pacific stresses are too zonal.
Surface Short Wave	1) N. Pacific and N. Atlantic regions have too much cloud and therefore too little short wave heating at the surface. 2) Excessive surface flux in the regions associated with marine strato-cumulus indicating too little cloud in these regions.	1) The excessive heating associated with the lack of marine stratocumulus cloud persists into this season. 2) Too much cloud, and therefore too little surface heating. in the central southern sub-tropical Pacific to the east of the SPCZ.
Surface Long Wave	1) Major differences are associated with the regions of too little marine stratocumulus cloud.	1) Major differences are associated with the regions of too little marine stratocumulus cloud.
Latent Heating	1) Tropical and sub-tropical evaporation is larger in the model compared to climatology by 20-50Wm^{-2}. 2) There are large differences associated with the Indian Monsoon.	1) Tropical and sub-tropical evaporation is larger in the model. 2) Exception to (1) is in the central equatorial regions where the low model winds lead to very low evaporation rates. 3) Large evaporation rates to the east of Australia which. in part, may be caused by the high model winds in this region.
Sensible Heating	1) The model sensible heat fluxes are typically 10-20Wm^{-2} rather than 0-10Wm^{-2} as indicated by the climatologies. This may be due to the model overestimation of the air-sea temperature difference. The contribution of the sensible heat flux to the total heating is not a dominant term.	1) As in summer. 2) There are larger significant differences in the sensible heat flux in the region of the Kuroshio and the Gulf Stream at this time of year when cold air moves over a much warmer sea.
SIGNIFICANT DIFFERENCES IN TOTAL HEATING	1) Too little heat entering the ocean in the north Pacific (dominated by short wave). 2) Too little heat entering the ocean in the south Pacific east of Australia (dominated by latent heat flux). 3) Too little heat entering the ocean to the east of the SPCZ (dominated by short wave). 4) Too much heating in the east Pacific (dominated by short wave). 5) Too little heating to the north and west of Australia (dominated by the latent heat flux).	1) Large differences associated with the warm waters of the Gulf Stream and Kuroshio (dominated by latent and sensible heat fluxes). 2) Too little heat entering the ocean in the south Pacific east of Australia (dominated by latent heat flux). 3) Too little heat entering the ocean to the east of the SPCZ (dominated by short wave). 4) Too much heating in the central equatorial Pacific (dominated by latent heat flux associated with low winds). 5) Too little heating associated with the Pacific NE trades (dominated by the latent heat flux).

TABLE 2: SUMMARY OF COMPARISON OF FLUX DIFFERENCES WITH FLUX CORRECTIONS

MAJOR FEATURE IN FLUX CORRECTION	CORRESPONDING FEATURE (IF ANY) IN FLUX DIFFERENCE
SUMMER	
Note: Flux correction features associated with regions of high horizontal SST gradient are not included as these inevitably show large values. See text for details.	
1. Heating in the North Pacific and North Atlantic.	1. The Pacific pattern matches well (ignoring the high values in the west associated with the high gradient SST) but not so well in the Atlantic. The flux differences are due to the model over-estimation of cloud in this region.
2. Strong heating in the central equatorial Pacific.	2. This does not show up in the flux differences. It is due to the too cold model SSTs on the equator (see text).
3. Heating to the east of Australia and in the central south sub-tropical Pacific.	3. This pattern matches well and is associated with the excess evaporation in these regions supplemented by too much cloud (too little surface short wave) in the eastern part.
4. Heating to the west of Australia in the Indian Ocean and in the Arabian Sea and Bay of Bengal.	4. These features also show up clearly in the flux difference largely being caused by the excessive evaporation in the model in these regions.
5. Large cooling in the far eastern equatorial Pacific.	5. Associated with the lack of marine cloud in these regions and also the underestimation of upwelling in the ocean model.
WINTER	
1. Cooling in the North East Pacific.	1. This does not show up in the flux differences and needs further investigation.
2. Heating in the central North Pacific.	2. The general pattern is similar with too much evaporation under the NE trades.
3. Heating in the South Pacific east of Australia.	3. There is too much cooling in this region associated with excessive evaporation.
4. Cooling in the equatorial central Pacific.	4. This shows up very clearly and is related to the light winds and low evaporation in this region.
5. Cooling off Africa just north of the equator in the Atlantic.	5. This feature is not present in the flux differences and needs further investigation. It may be associated with the strong upwelling in this region.

REFERENCES

Berliand, M.E. and T.G. Berliand, 1952. Determining the net long wave radiation of the Earth with consideration of the effect of cloudiness. Isv. Akad Nauk. SSSR Ser. Geofis, No 1.

Bunker,A.F. 1976. Computations of surface energy flux and annual air sea interaction cycles of the North Atlantic Ocean. Mon.Weath. Rev., 104,1122-1140.

Cullen, M., 1993. The unified forecast/climate model. Met. Mag (UK), 1449, 81-94.

Esbensen, S.K. and Y. Kushnir, 1981. The heat budget of the global ocean: An atlas based on estimates from surface marine observations. Climate Research Institute Report No. 29, Oregon State University, Corvallis, 27pp.

Foreman, S.J., O. Alves and N. Brooks, 1994. Assessment of surface fluxes from NWP systems. Forecasting Research Division Technical Note No. 104, Meteorological Office, Bracknell, UK.

Gordon,C., 1988. A study of air-sea interaction in the tropical Pacific with a coupled GCM. In 'Modelling the Sensitivity and Variations of the Ocean-Atmosphere System', WMO/TD No.254, pp. 262-270.

Hadley Centre, 1995. Modelling Climate Change 1860-2050. Available from the Hadley Centre.

Haney,R.L., 1971. Surface thermal boundary conditions for ocean circulation models. J. Phys. Oceanogr. 1, 241-248.

Harrison,D.E., 1989. On climatological monthly mean wind stress and wind stress curl fields over the World Ocean. J. Clim., 2,57-70.

Hellerman,S. and M. Rosenstein, 1983. Normal monthly wind stresses over the world ocean with error estimates. J. Phys. Oceanogr., 13,1093-1104.

Kent,E.C. and P.K. Taylor, 1995. A comparison of sensible and latent heat flux estimates for the North Atlantic Ocean. (Submitted for publication.)

Large,W.G., and S. Pond, 1981. Open ocean momentum flux measurements in moderate to strong winds. J. Phys. Oceanogr., 11,324-336.

Large,W.G., and S. Pond, 1982. Sensible and latent heat flux measurements over the sea. J. Phys. Oceanogr., 11, 324-336.

Legates, D.R., and C.J. Willmott, 1990. Mean seasonal and spatial variability in gauge corrected global precipitation. International J. Clim. 10, 111-127.

Manabe, S., Stouffer, R.J., Spelman, M.J. and K. Bryan, 1991. Transient responses of a coupled ocean-atmosphere model to gradual changes of atmospheric CO_2. Part I: Annual mean response. J. Climate,4,785-818.

Miller, M.J., A.C.M. Beljaars, and T.N. Palmer, 1992. The sensitivity of the ECMWF model to the parametrization of evaporation from the tropical oceans. J. Climate 5, 418-434.

Mitchell,J.F.B., 1977. Some experiments using a simple oceanic mixed layer model. MetO20, Dynamical Climatology Technical Note II/86 (UK Met. Office).

Murphy, J.M. (1995) Transient response of the Hadley Centre coupled ocean-atmosphere model to increasing carbon dioxide. Part I: Control climate and flux adjustment. Journal of Climate, 8, 36-56.

Oberhuber,J.M., 1988. An atlas based on the 'COADS' data set: the budgets of heat, buoyancy and turbulent kinetic energy at the surface of the global ocean. Max-Planck Institute for Meteorology, Hamburg. Report 15.

Quinn,W.H. and W.V. Burt. 1968. Computation of incoming solar radiation over the Equatorial Pacific. J. Appl. Met., 7, 490-498.

Reed, R.K., 1977. On estimating insolation over the ocean. J. Phys.Oceanogr., 6, 781-800.

Roberts, C.M. and C. Gordon, 1995. Flux corrections in coupled models. (In preparation).

Sausen, R., K. Bartel and K. Hasselman, 1988. Coupled ocean-atmosphere models with flux correction. Climate Dynamics,2,145-163.

Smith, R.N.B., 1993. Subsurface, surface and boundary layer processes. Unified Model Documentation Paper No. 24.

Woodruff, S.D., R.J. Slutz, R.L Jenne and Steurer, 1987. A comprehensive ocean-atmosphere data set. Bull. Amer. Met. Soc., 68,1239-1250.

Wright, P., 1988. An atlas based on the 'COADS' data set: Fields of mean wind, cloudiness and humidity at the surface of the global ocean. Max-Planck institute for Meteorology, Hamburg. Report 14.

Zillmann, J.W., 1972. A study of some aspects of the radiation and the heat budgets of the southern hemisphere oceans. Meteorol.Stud., 26, Bur. of Meteorol., Dept. of the Interior, Canberra, Australia, 562pp.

FIGURE CAPTIONS

In all figures a summer mean is over the months June, July and August (Northern Hemisphere summer) and a winter mean over the months December, January, February (Northern Hemisphere winter).

Figure 1: a: Unified model summer windstress (Nm^{-2}).
b: Hellerman and Rosenstein summer windstress (Nm^{-2}).
c: Difference in magnitude of the summer wind stress (a)-(b).
d: Unified model September windstress in the east Pacific (Nm^{-2}).
e: Hellerman and Rosenstein windstress in the east Pacific(Nm^{-2}).

Figure 2: a: Unified model winter windstress (Nm^{-2}).
b: Hellerman and Rosenstein winter windstress (Nm^{-2}).
c: Difference in magnitude of the winter wind stress (a)-(b).

Figure 3: a: Unified model summer short wave at surface (Wm^{-2}).
b: Oberhuber summer short wave at surface (Wm^{-2}).
c: Difference in the summer short wave at surface.

Figure 4: a: Unified model summer planetary albedo minus ERBE (1985-87) value.
b: Unified model winter planetary albedo minus ERBE (1985-87) value.

Figure 5: a: Unified model winter short wave at surface (Wm^{-2}).
b: Oberhuber winter short wave at surface (Wm^{-2}).
c: Difference in the winter short wave at surface.
d: Unified model total summer precipitation ($mmday^{-1}$).
e: Legates and Willmott total summer precipitation ($mmday^{-1}$).

Figure 6: a: Unified model summer net surface longwave radiation (Wm^{-2}).
b: Oberhuber summer net surface longwave radiation (Wm^{-2}).
c: Difference in the surface summer net long wave radiation.

Figure 7: a: Unified model winter net longwave radiation (Wm^{-2}).
b: Oberhuber winter net longwave radiation (Wm^{-2}).
c: Difference in the surface winter net longwave radiation.

Figure 8: a: Unified model summer latent heat flux (Wm^{-2}).
b: Oberhuber summer latent heat flux (Wm^{-2}).
c: Difference in the summer latent heat flux.

Figure 9: As fig.8 but for winter

Figure 10: a: The unified model latent heat transfer coefficient C_E as a function of Richardson number for different wind speeds.
b: The Oberhuber latent heat transfer coefficient C_E as a function of Richardson number for different wind speeds.

(The Richardson number is inversely proportional to the square of the wind speed so for a fixed wind speed increasing (negative) Ri_B implies increasing boundary layer instability - see the Appendix for further details.)

Figure 11: a: Unified model summer sensible heat flux (Wm^{-2}).
b: Oberhuber summer sensible heat flux (Wm^{-2})
c: Difference in the summer sensible heat flux

Figure 12: As fig.11 but for winter.

Figure 13: a: Unified model summer net surface heating (Wm^{-2}).
b: Oberhuber summer net surface heating (Wm^{-2}).
a: Difference in net surface heating.

Figure 14: As fig.13 but for winter.

Figure 15: a: Difference in summer net surface heating between the Oberhuber and Esbensen and Kushnir climatologies (Wm^{-2}).
b: Difference in winter net surface heating between the Oberhuber and Esbensen and Kushnir climatologies (Wm^{-2}).

Figure 16: a: Coupled model summer flux correction (Wm^{-2}).
b: Coupled model winter flux correction (Wm^{-2}).

Fig 1a

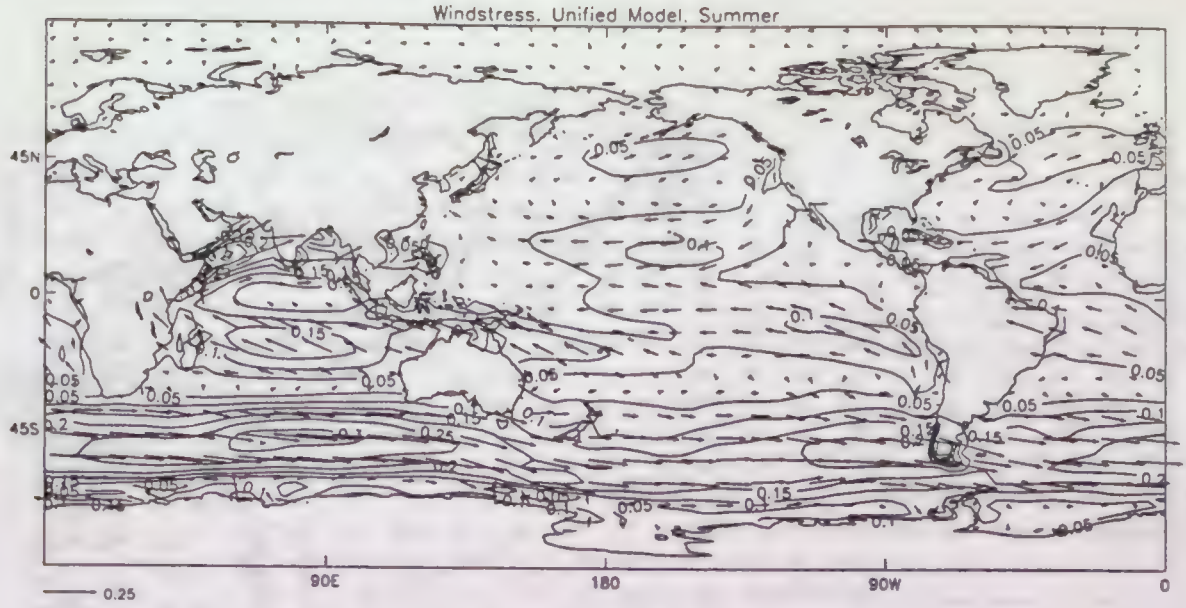

Fig 1b

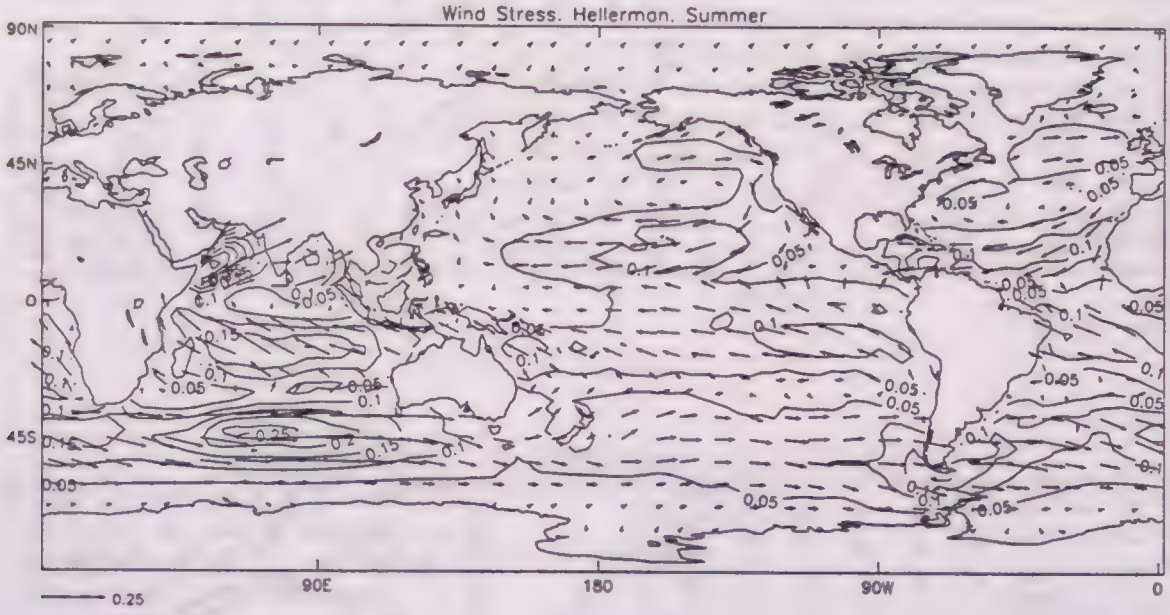

Fig 1c

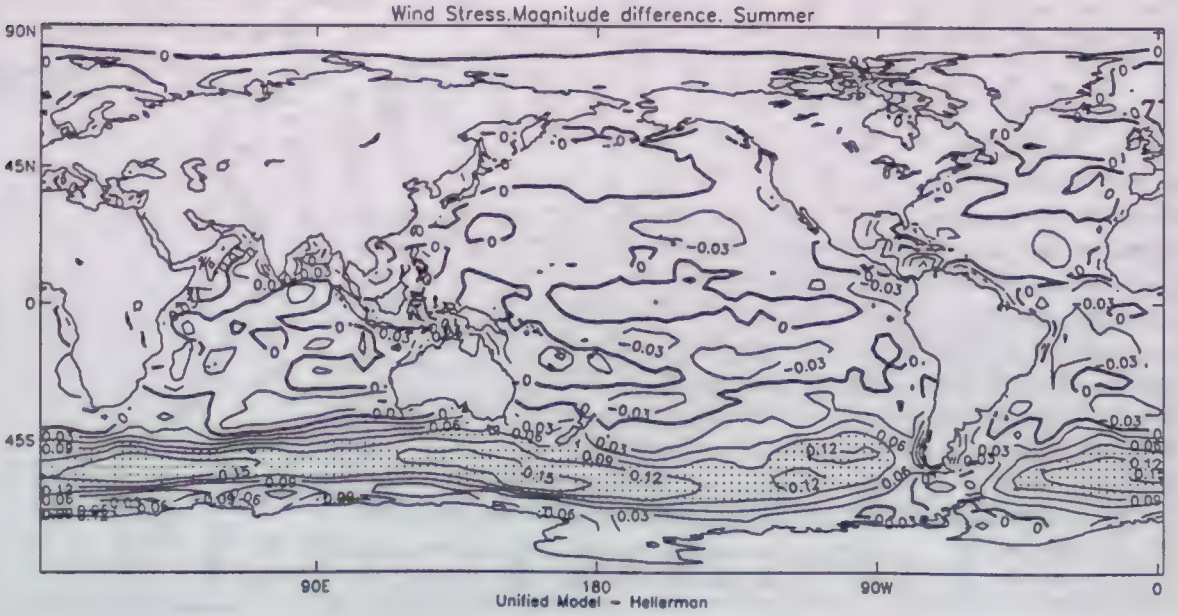

Fig 1d

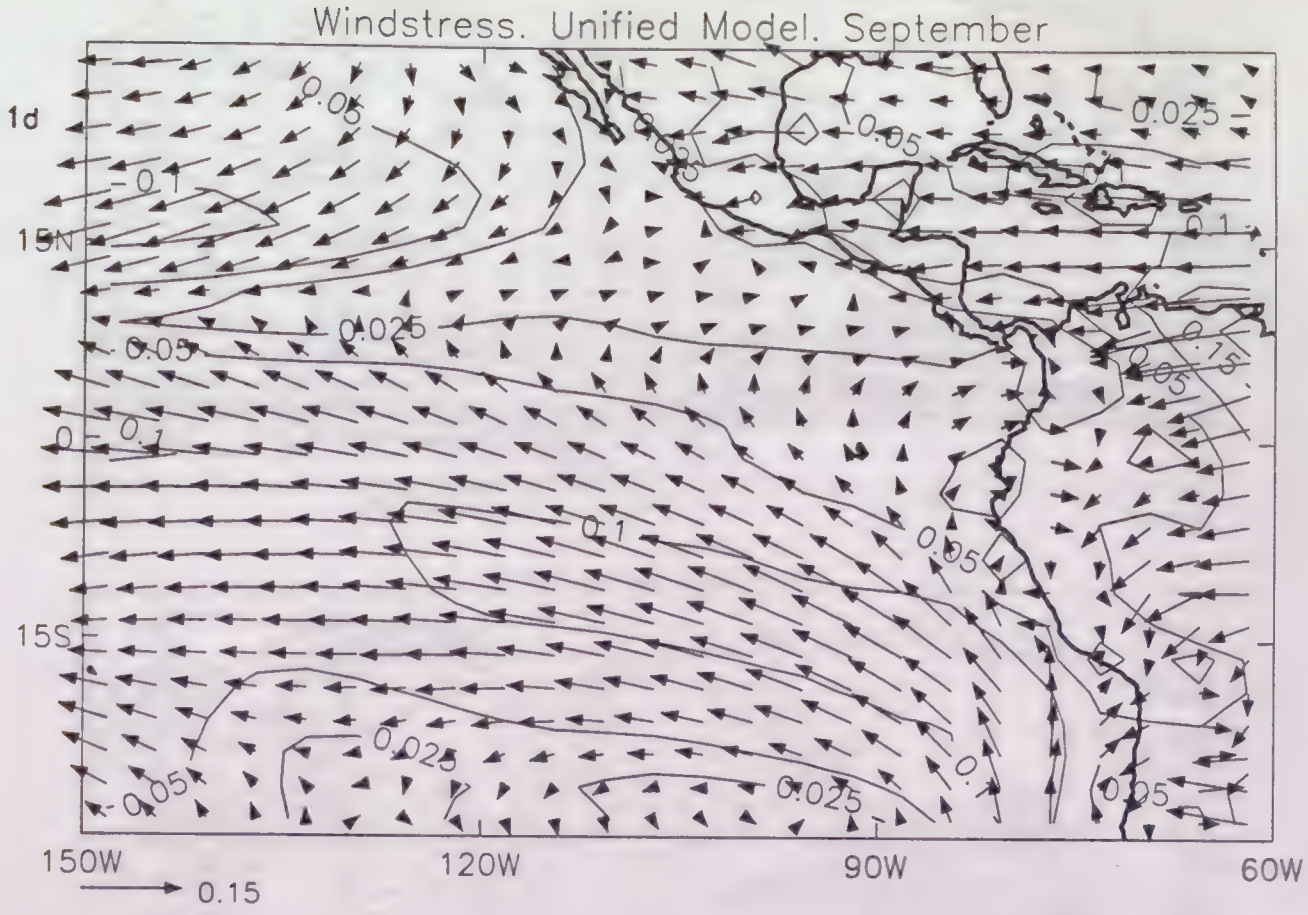
Windstress. Unified Model. September
15N
0
15S
150W
120W
90W
60W
0.15

Fig 1e

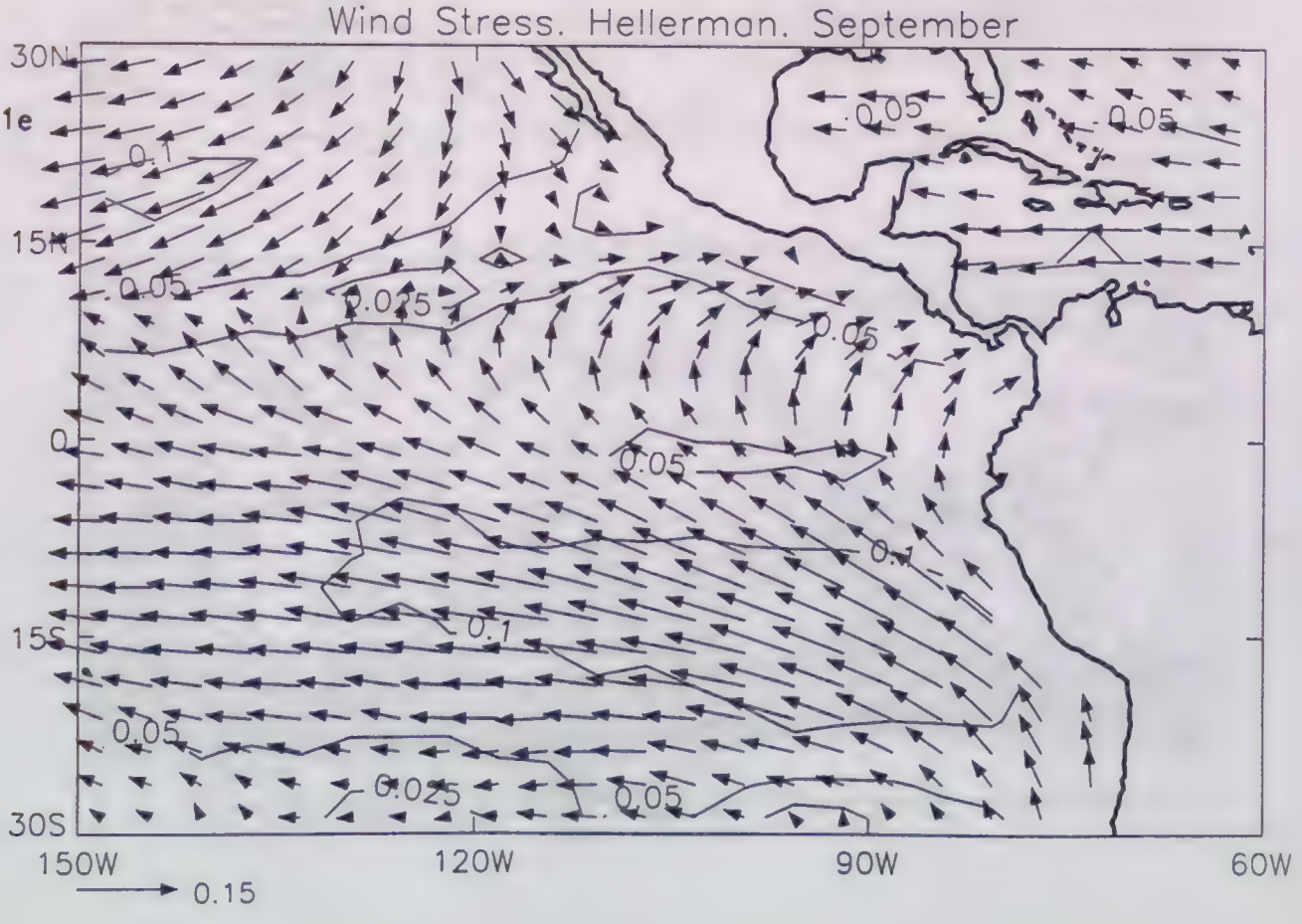
Wind Stress. Hellerman. September
30N
15N
0
15S
30S
150W
120W
90W
60W
0.15

Fig 2a

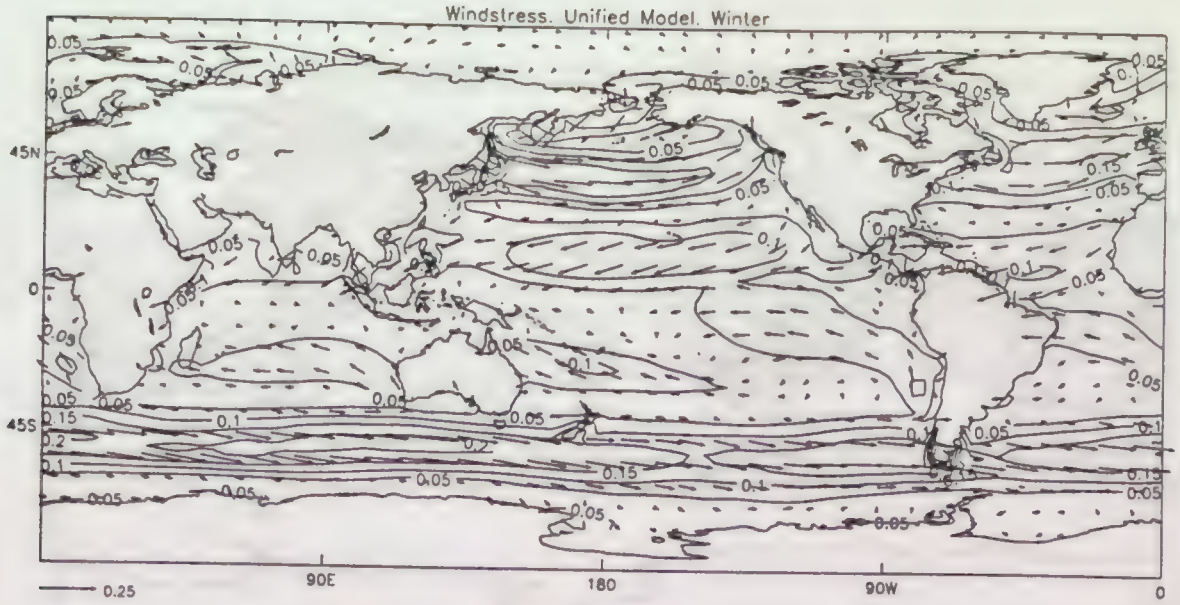

Fig 2b

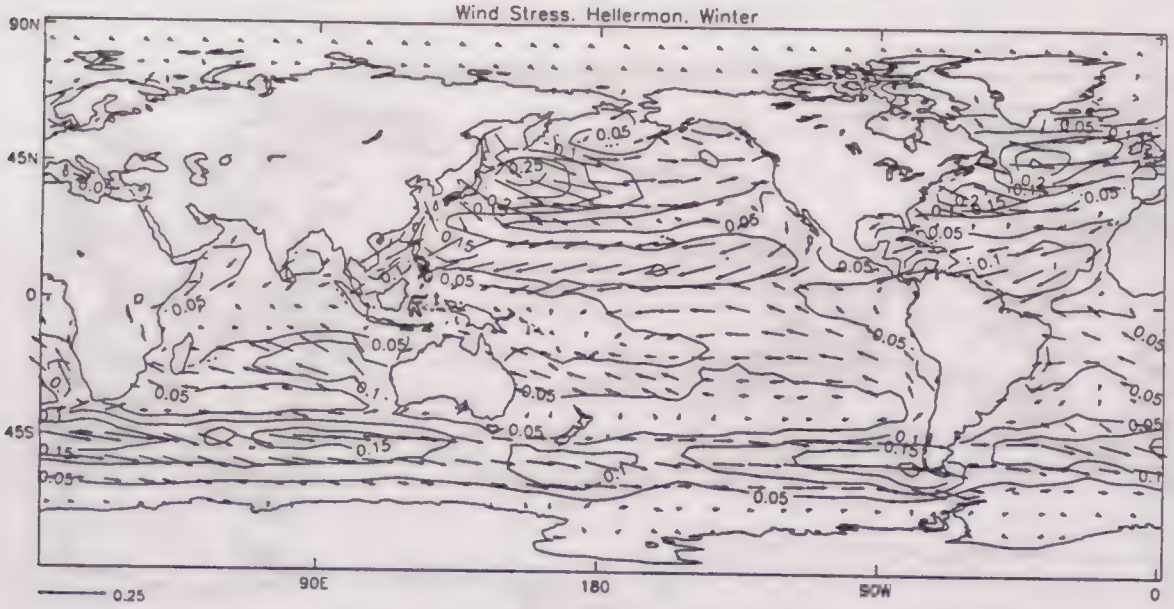

Fig 2c

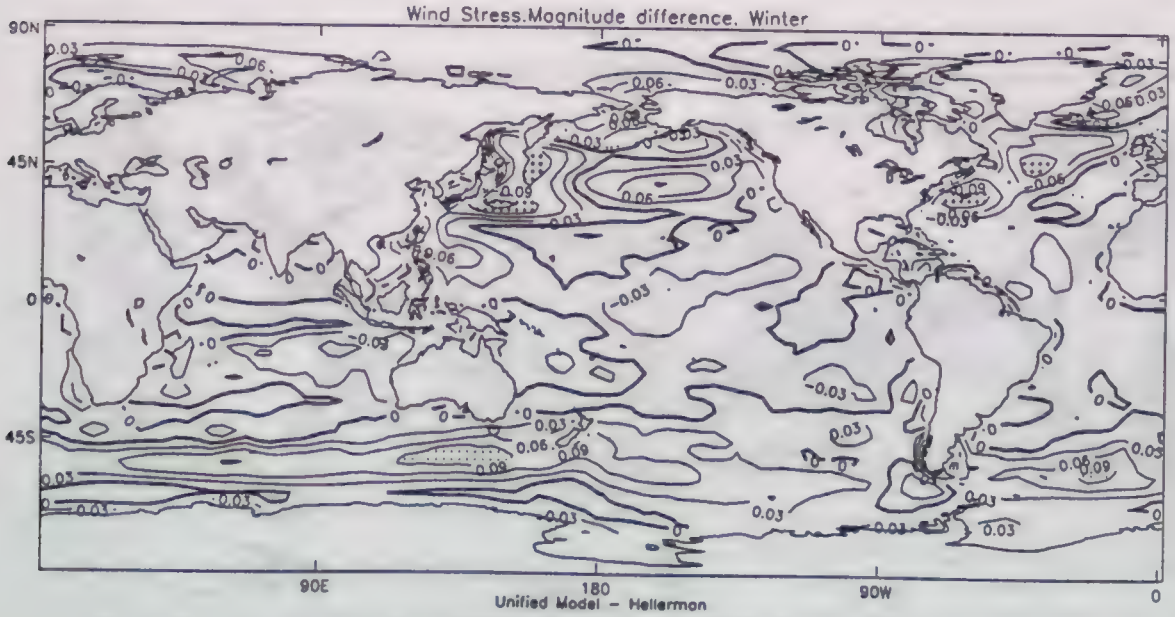

Fig 3a

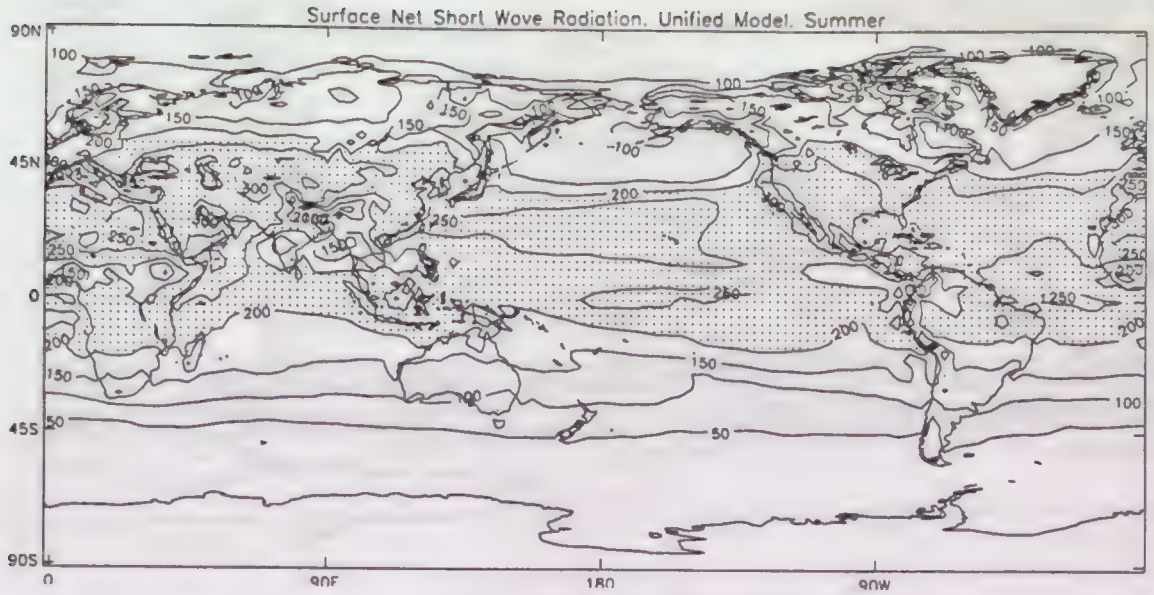

Fig 3b

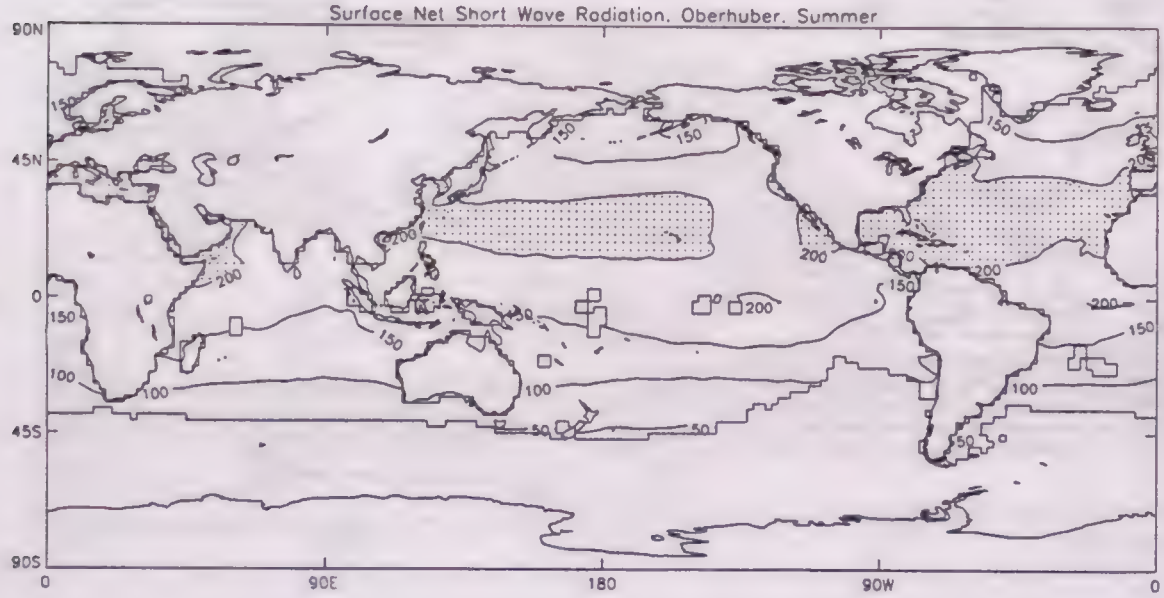

Fig 3c

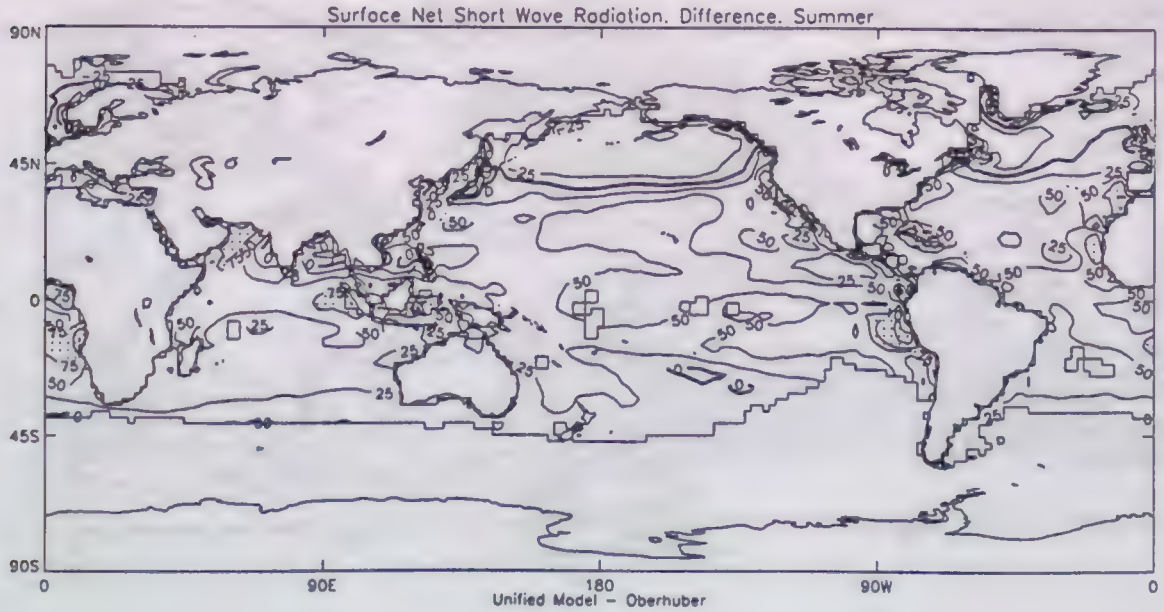

Fig 4a

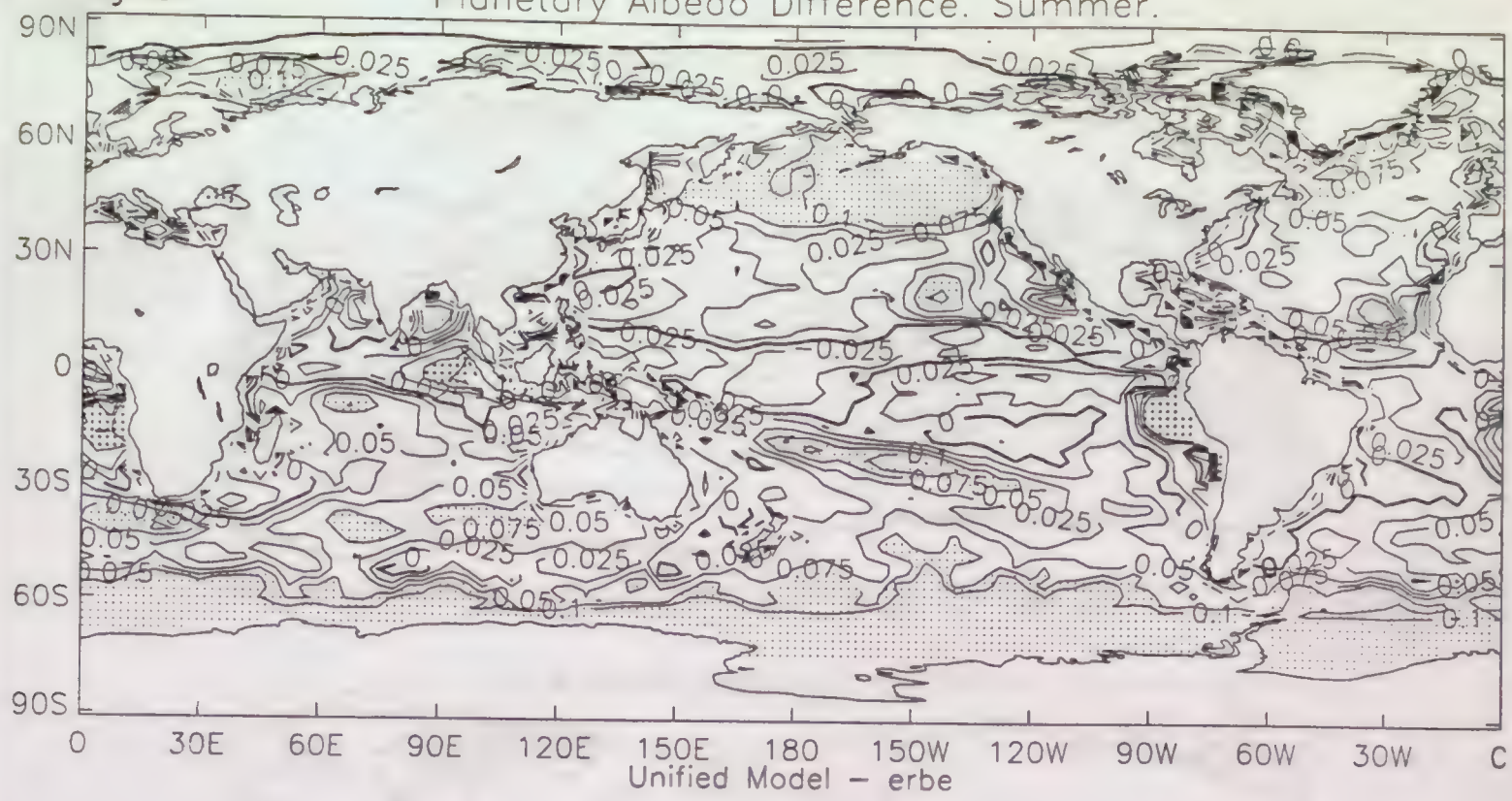
Planetary Albedo Difference. Summer.
90N
60N
30N
0
30S
60S
90S
0
30E
60E
90E
120E
150E
180
150W
120W
90W
60W
30W
Unified Model – erbe

Fig 4b

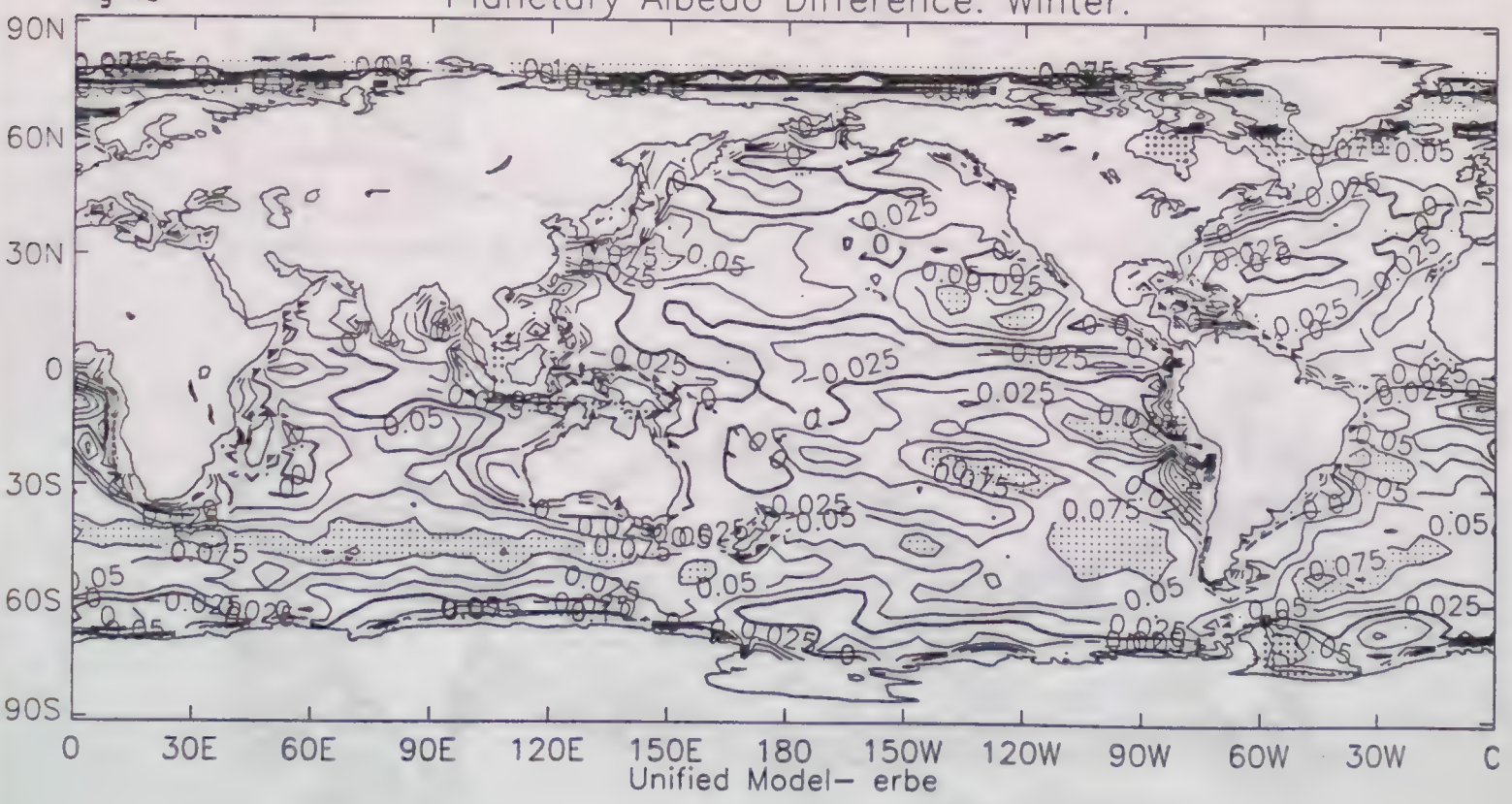
Planetary Albedo Difference. Winter.
90N
60N
30N
0
30S
60S
90S
0
30E
60E
90E
120E
150E
180
150W
120W
90W
60W
30W
Unified Model– erbe

Fig 5a

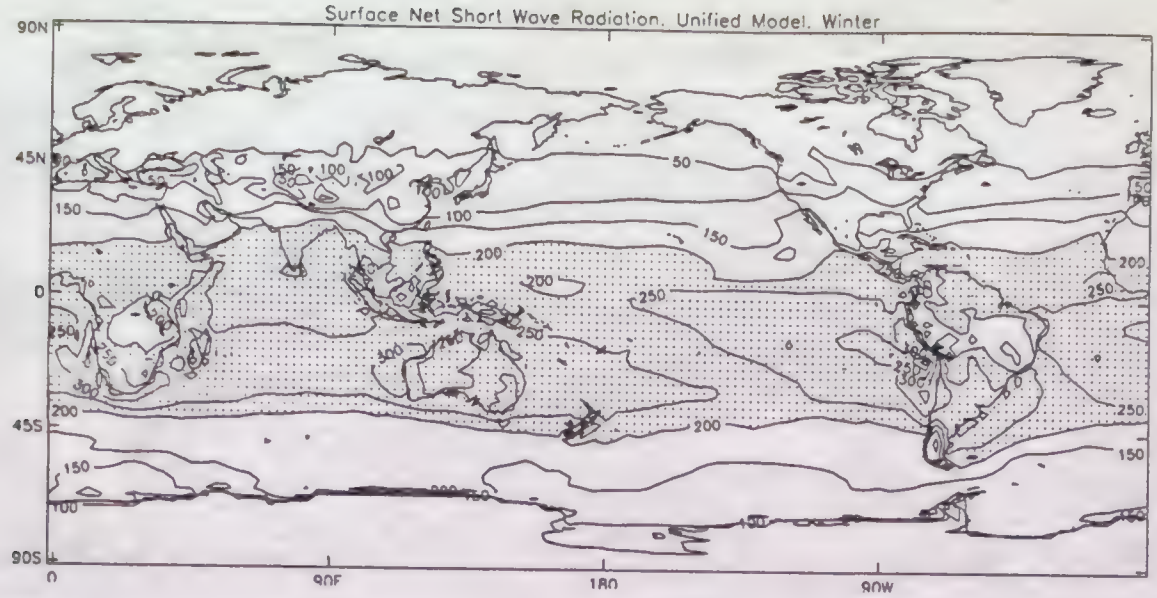

Fig 5b

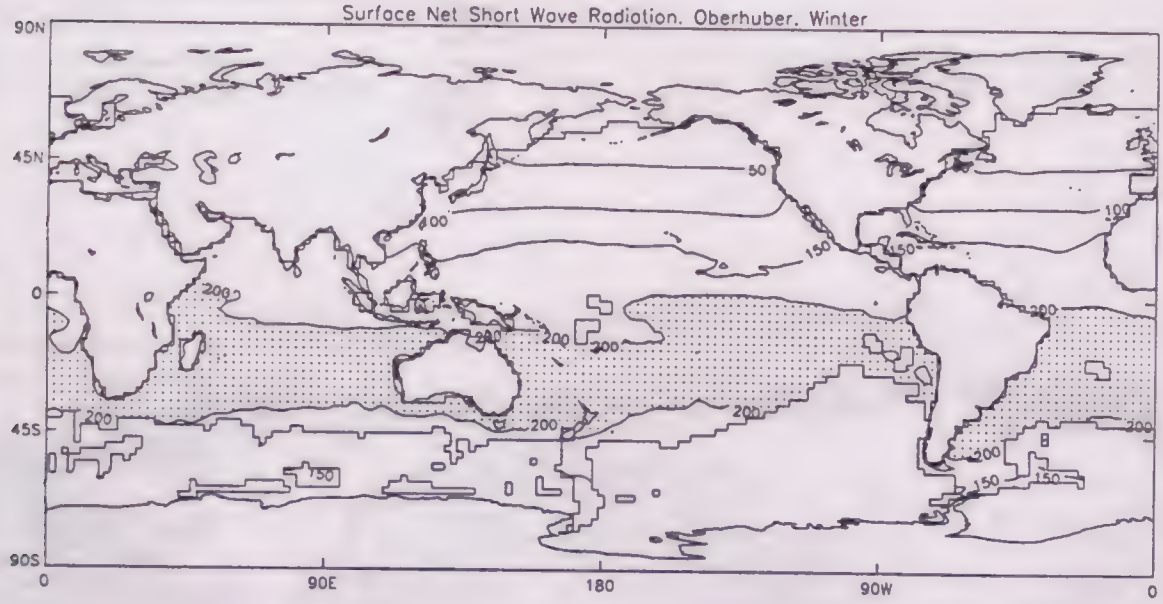

Fig 5c

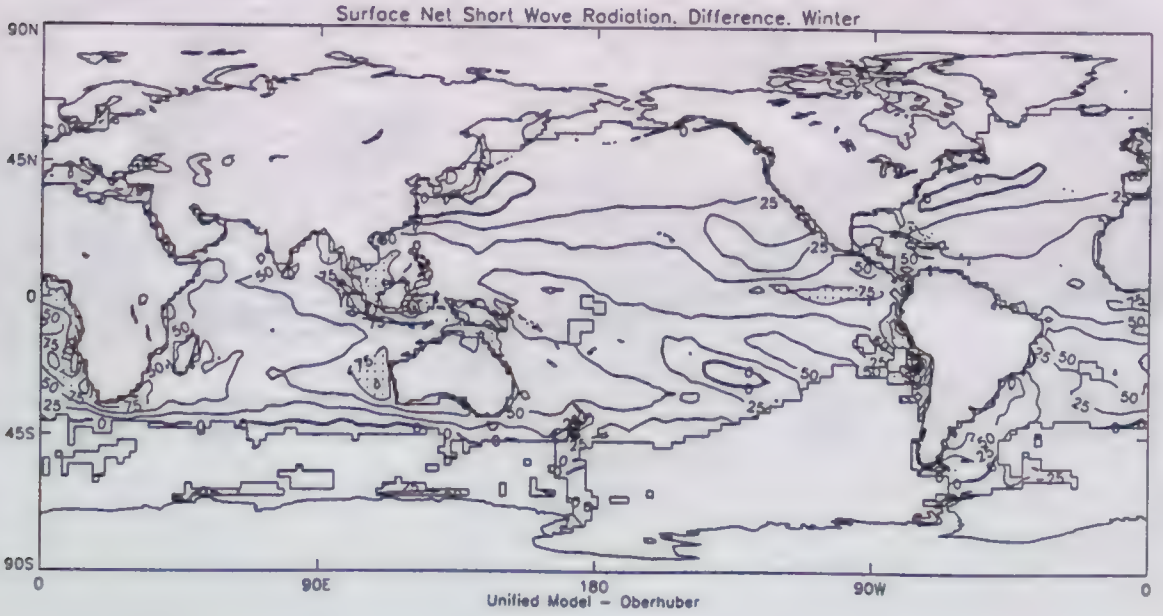

Fig 5d

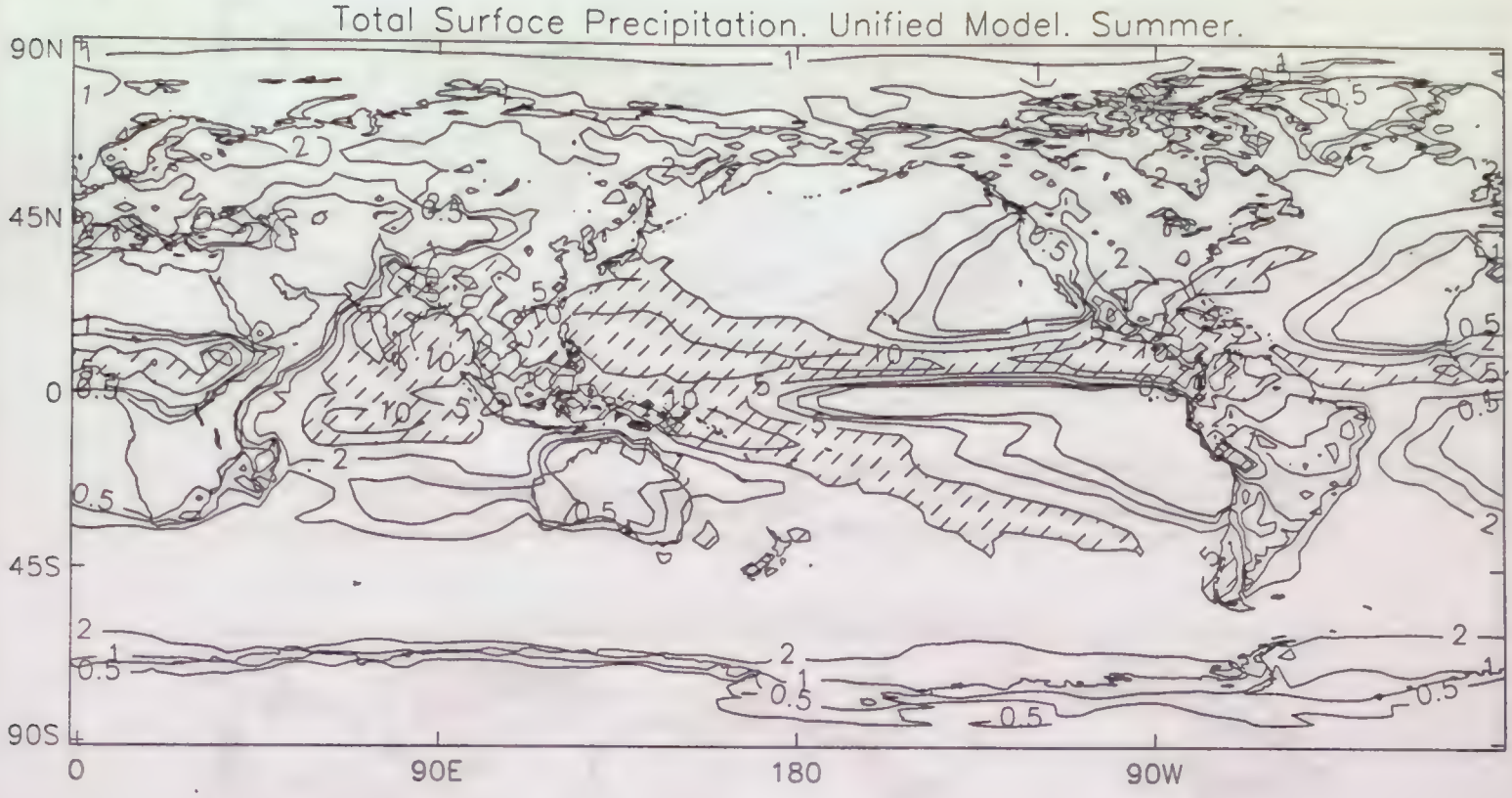
Total Surface Precipitation. Unified Model. Summer.
90N
45N
0
45S
90S
0
90E
180
90W

Fig 5e

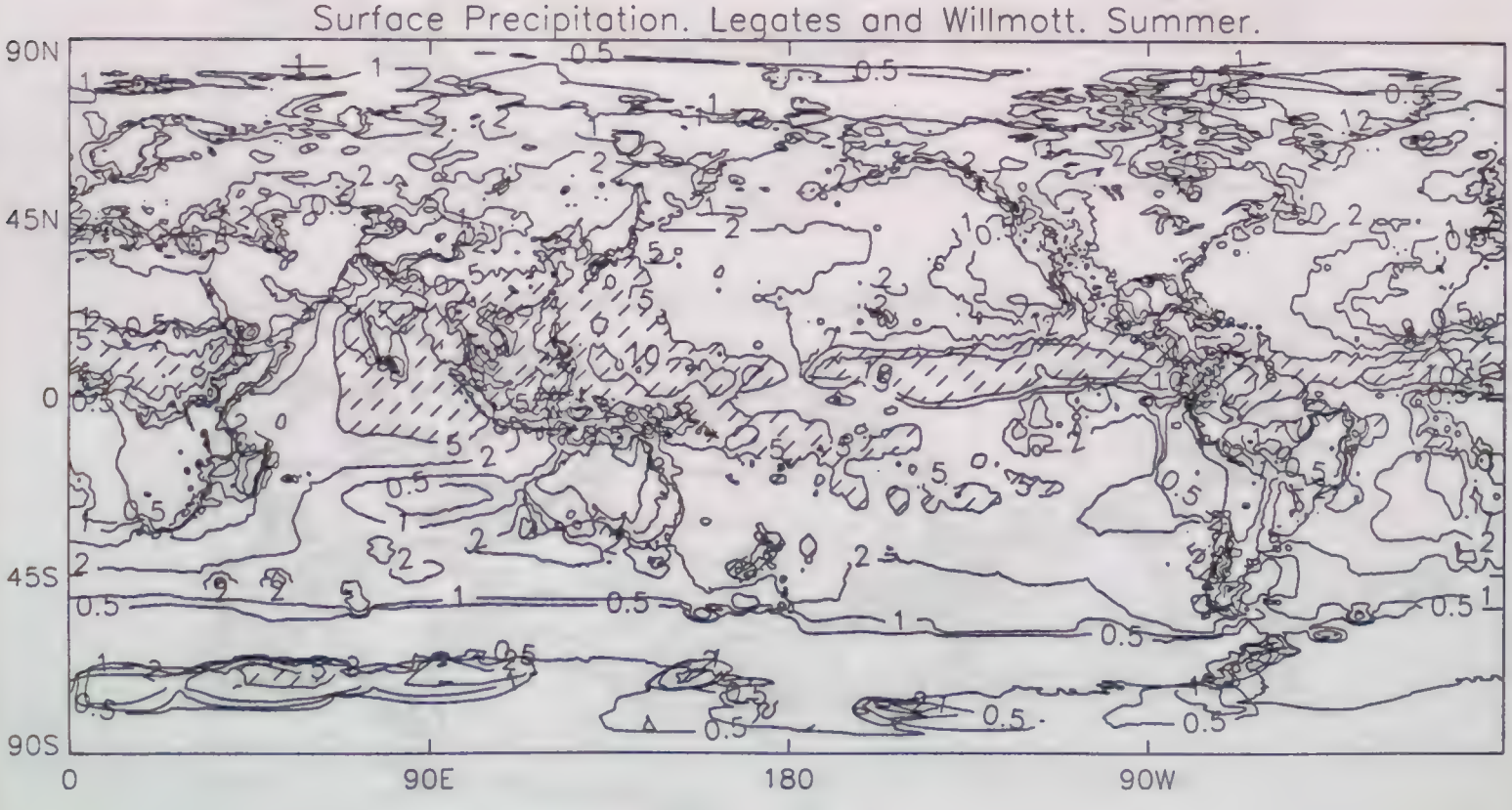
Surface Precipitation. Legates and Willmott. Summer.
90N
45N
0
45S
90S
0
90E
180
90W

Fig 6a

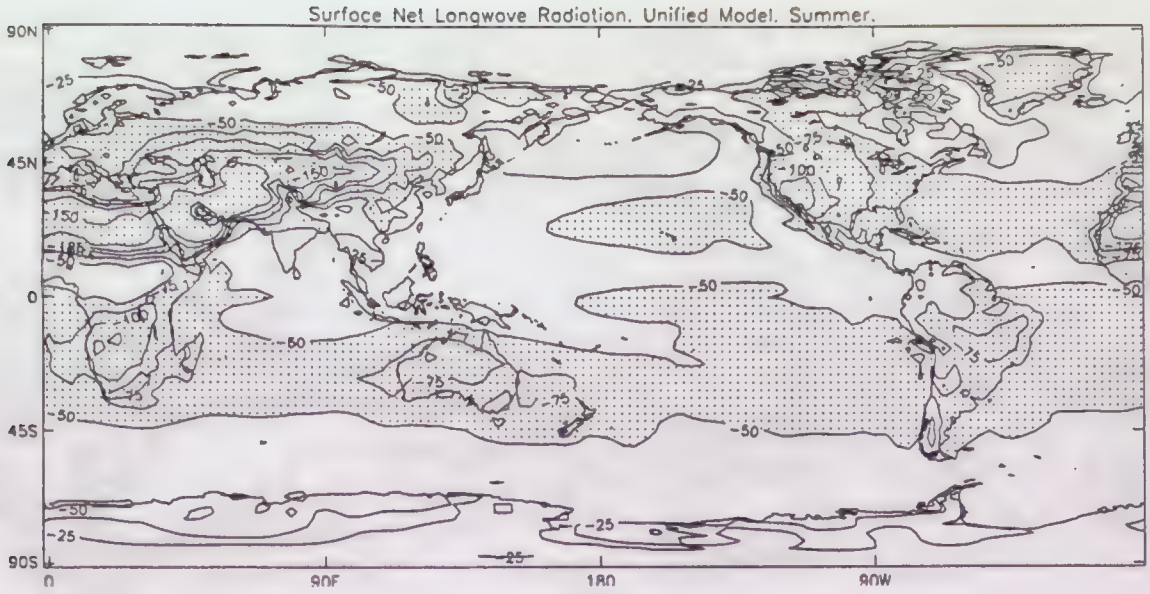

Fig 6b

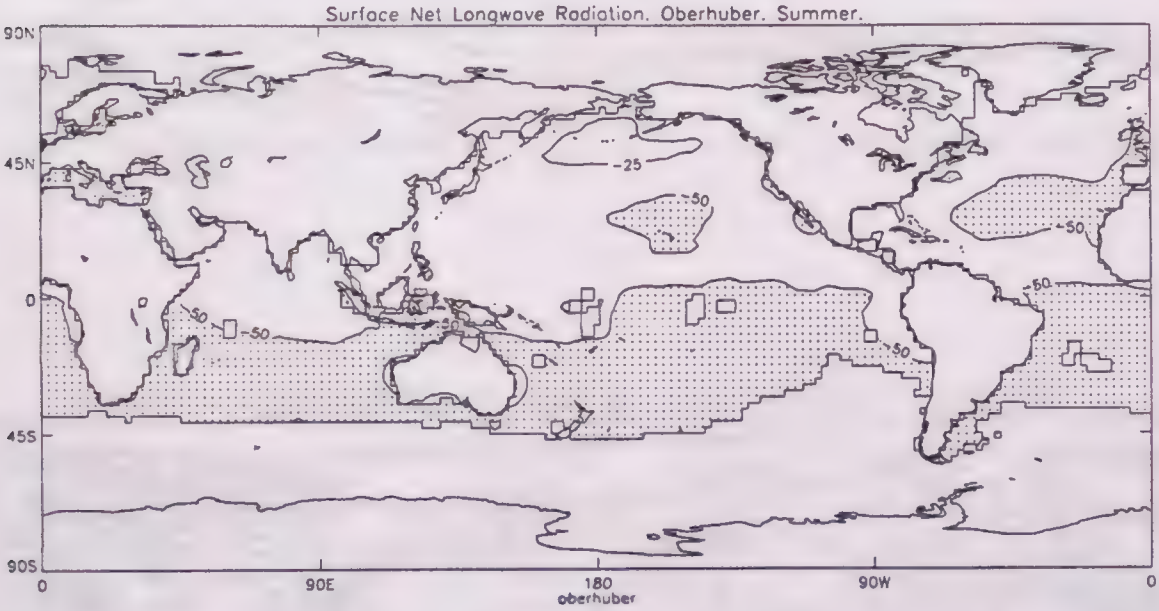

Fig 6c

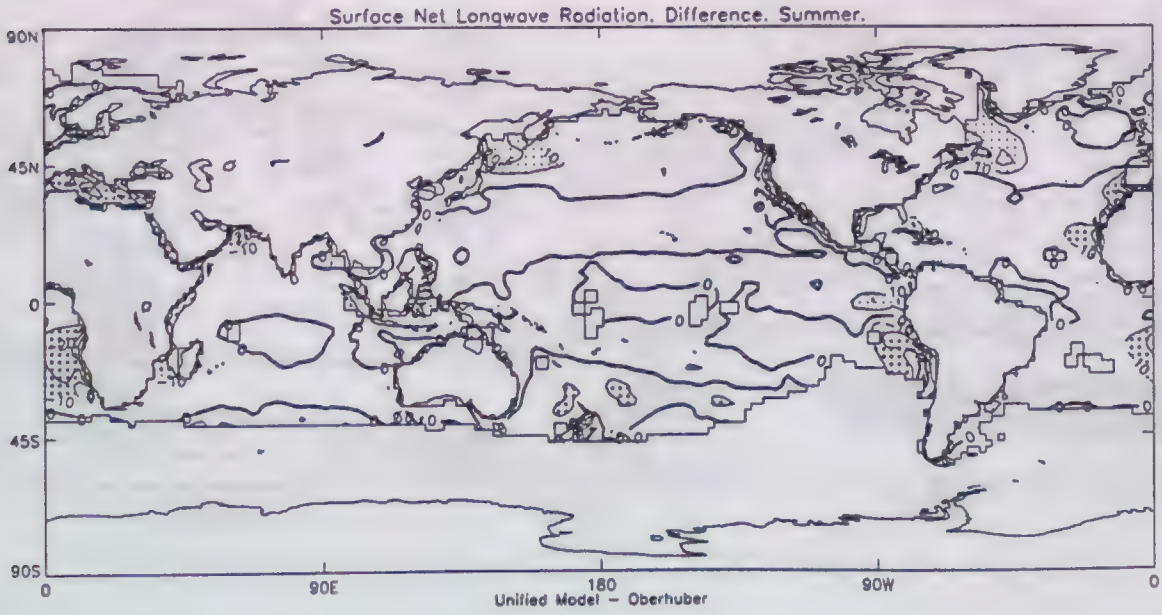

Fig 7a

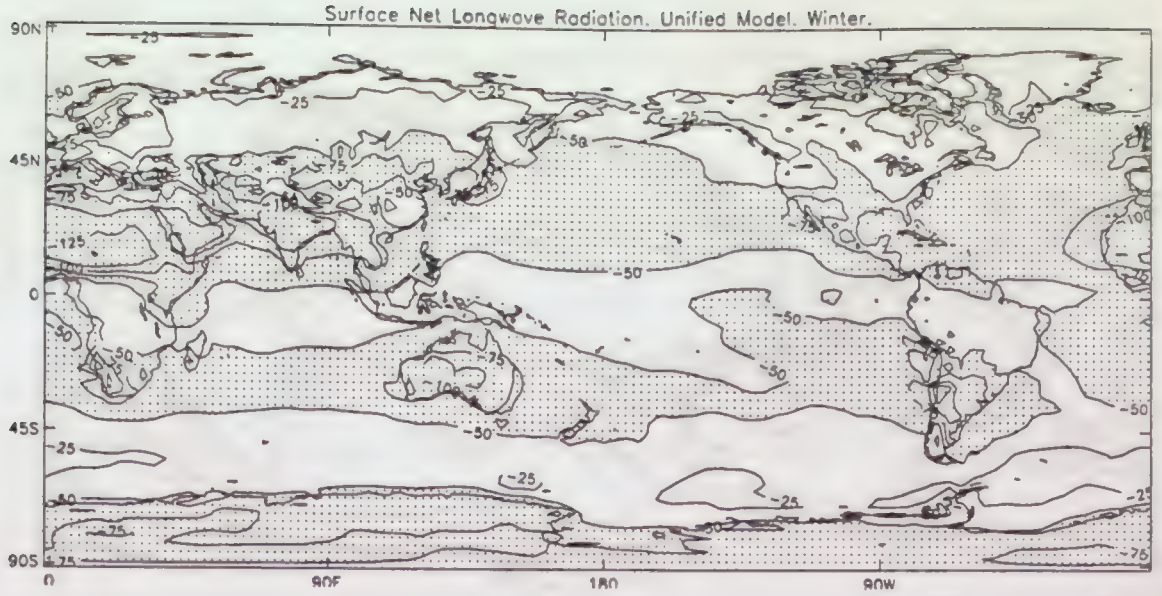

Fig 7b

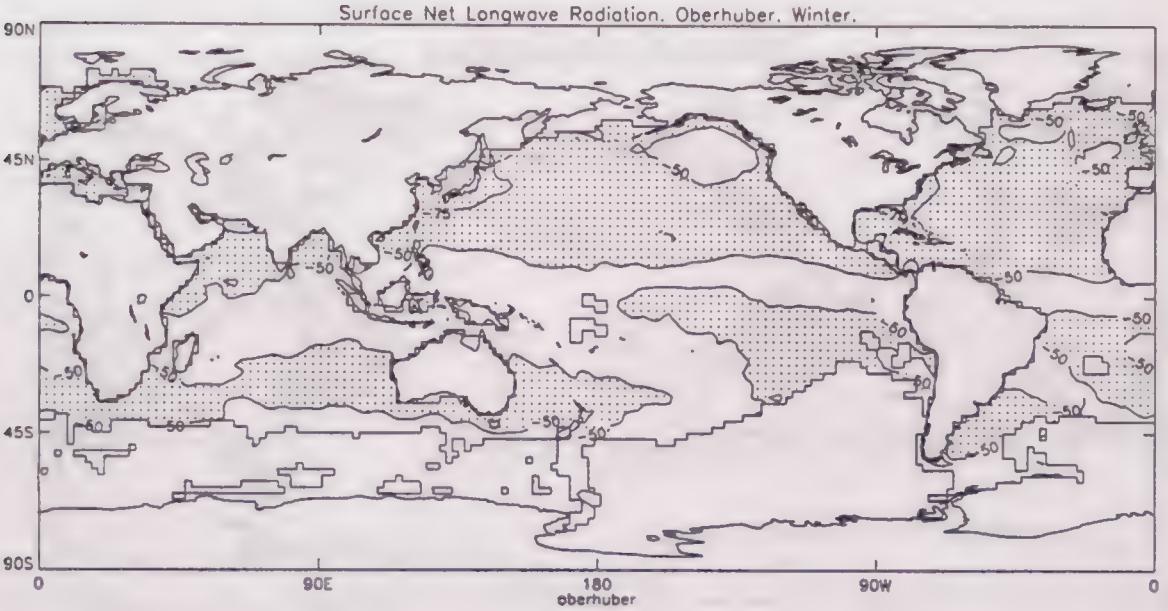

Fig 7c

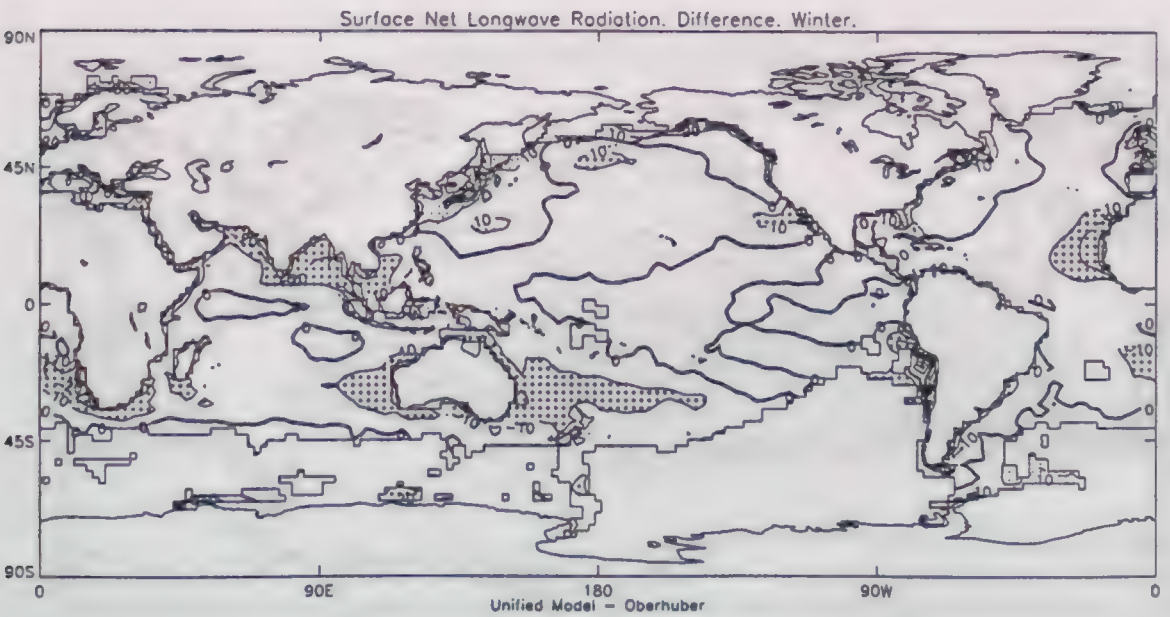

Fig 8a

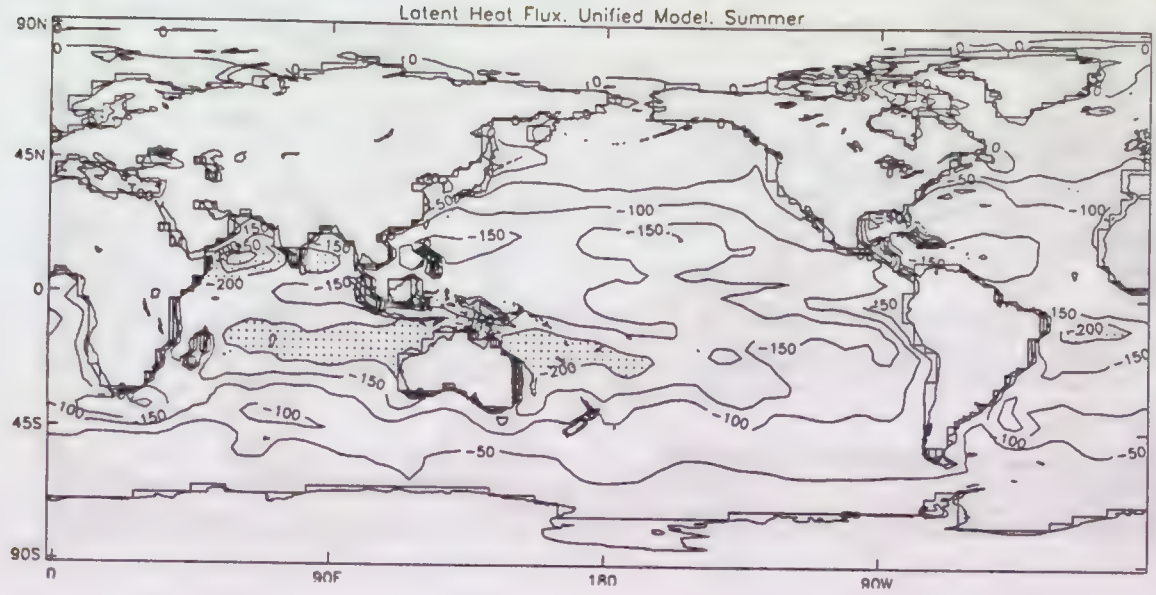

Fig 8b

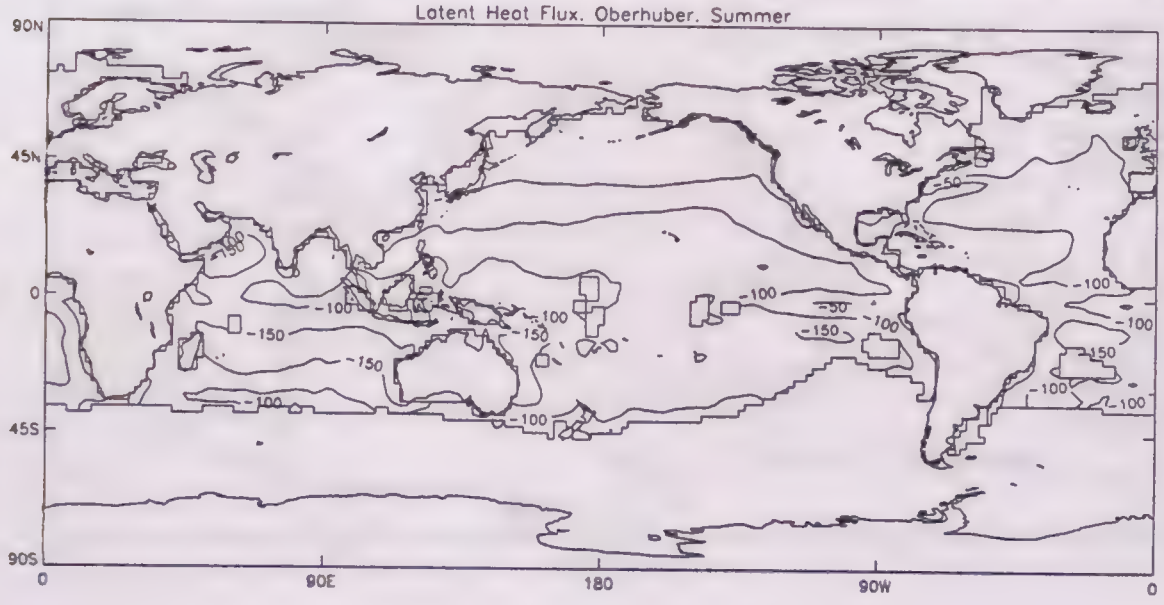

Fig 8c

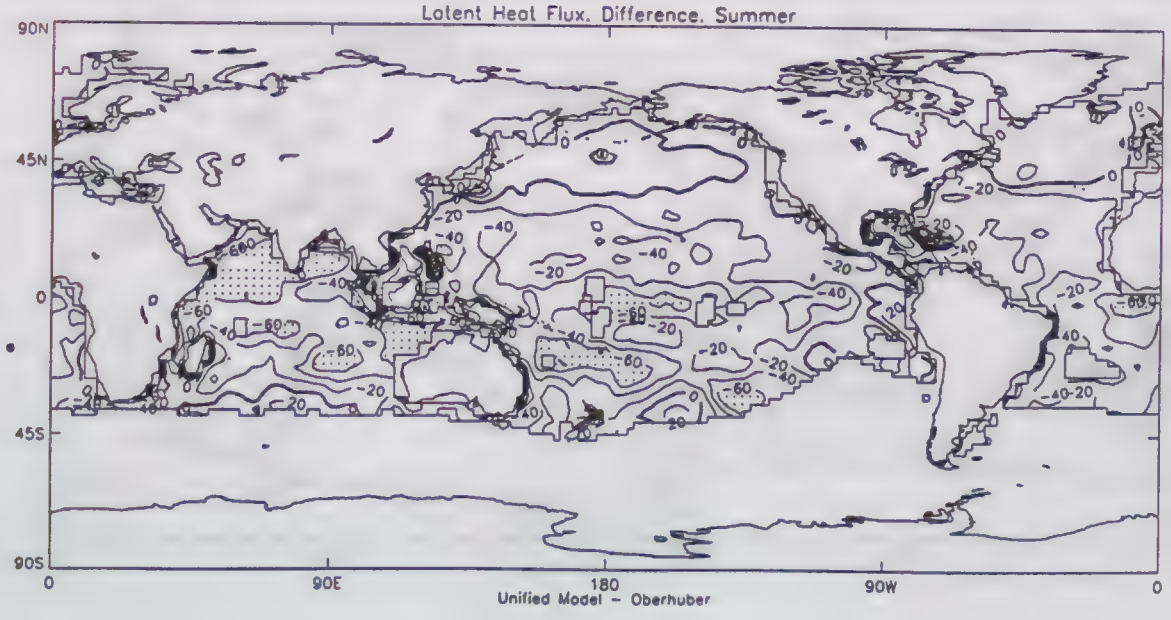

Fig 9a

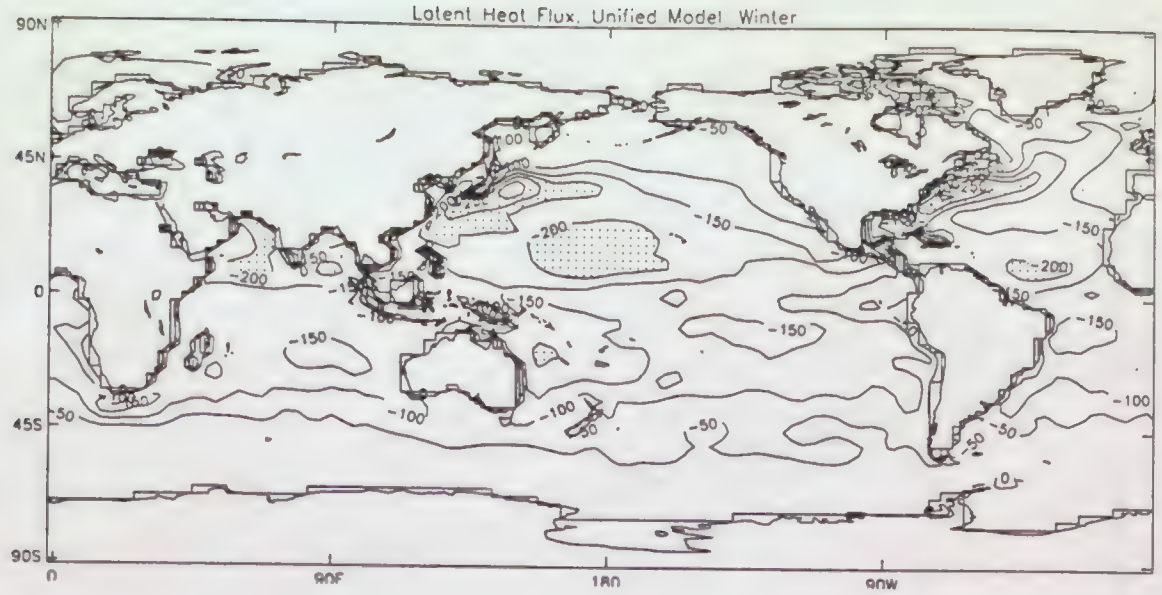

Fig 9b

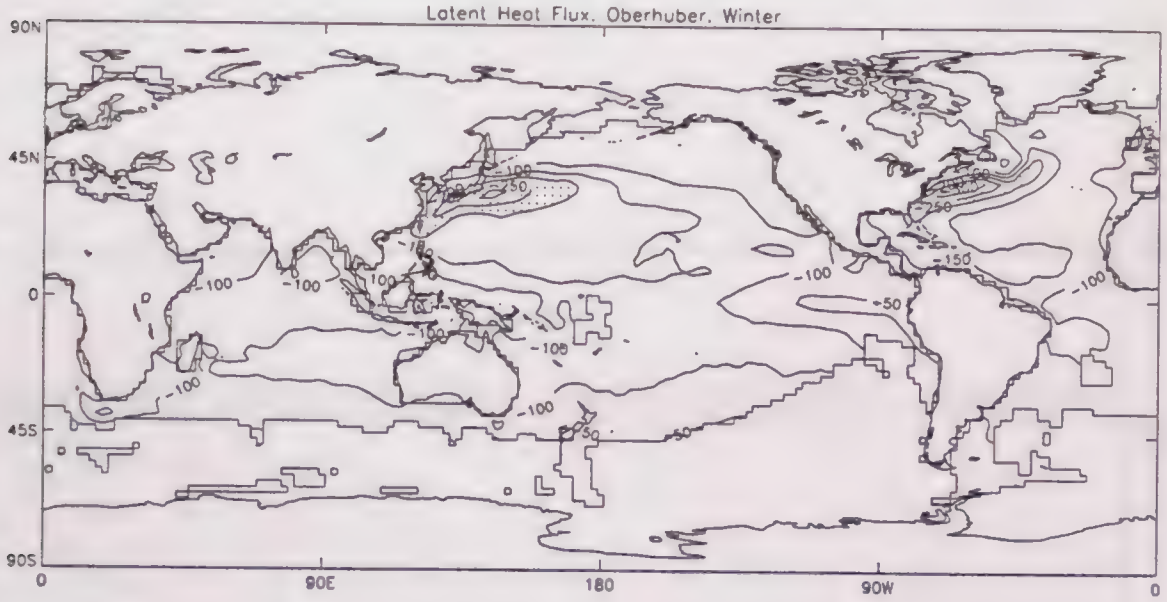

Fig 9c

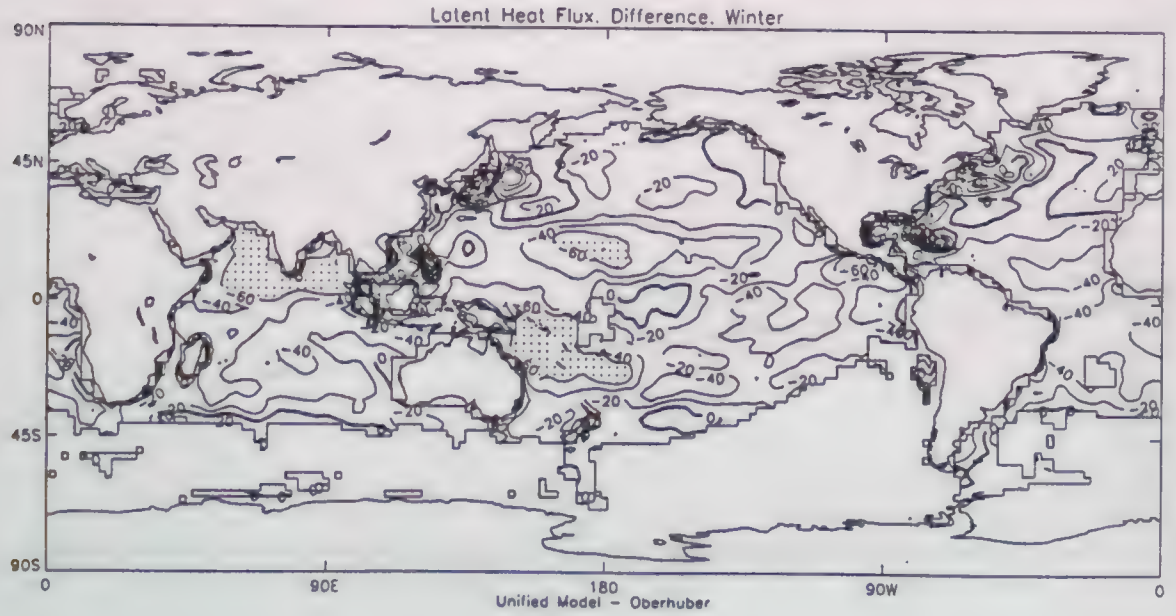

Fig 10

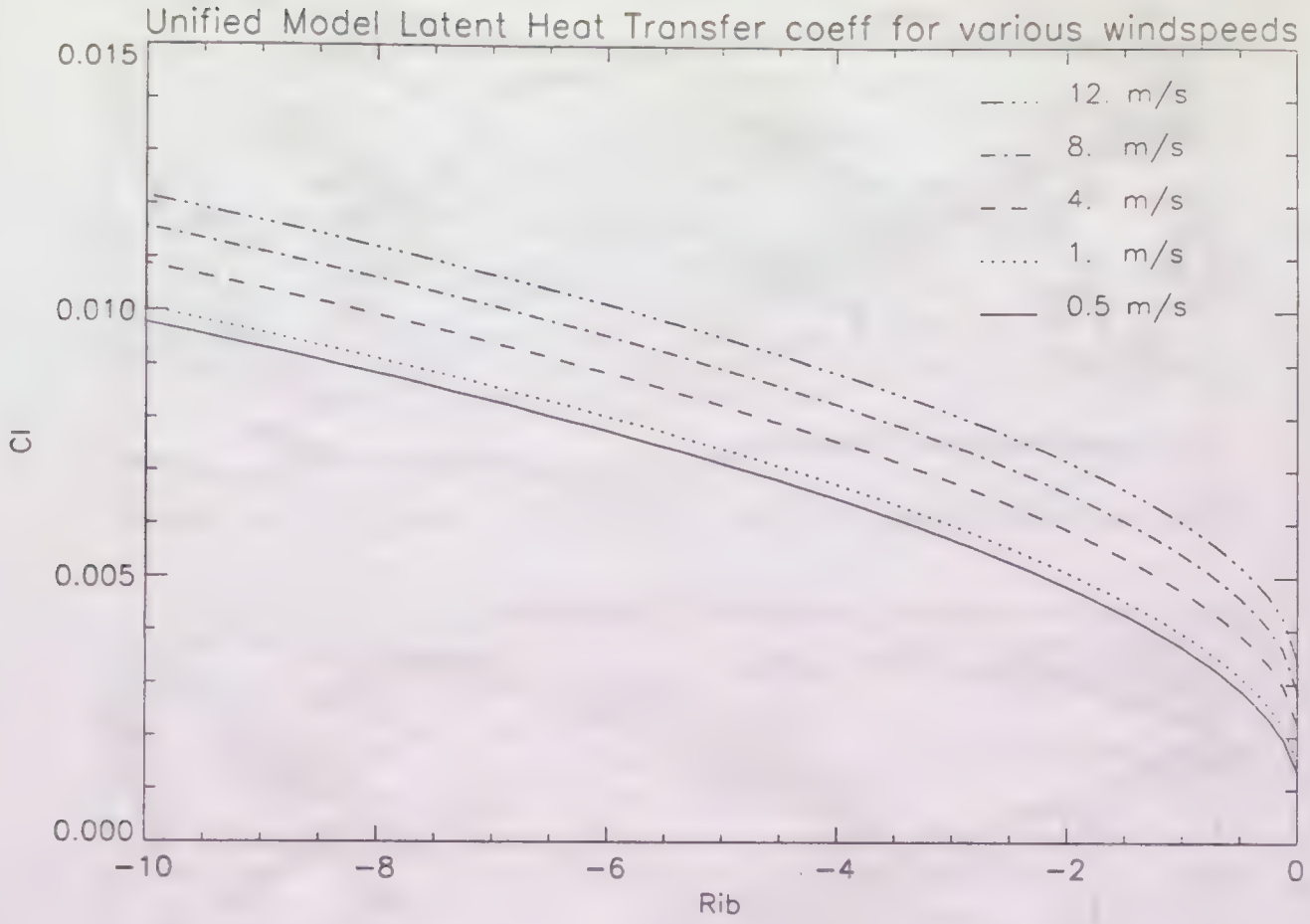
Unified Model Latent Heat Transfer coeff for various windspeeds
0.015
0.010
0.005
0.000
CI
12. m/s
8. m/s
4. m/s
1. m/s
0.5 m/s
−10
−8
−6
−4
−2
0
Rib

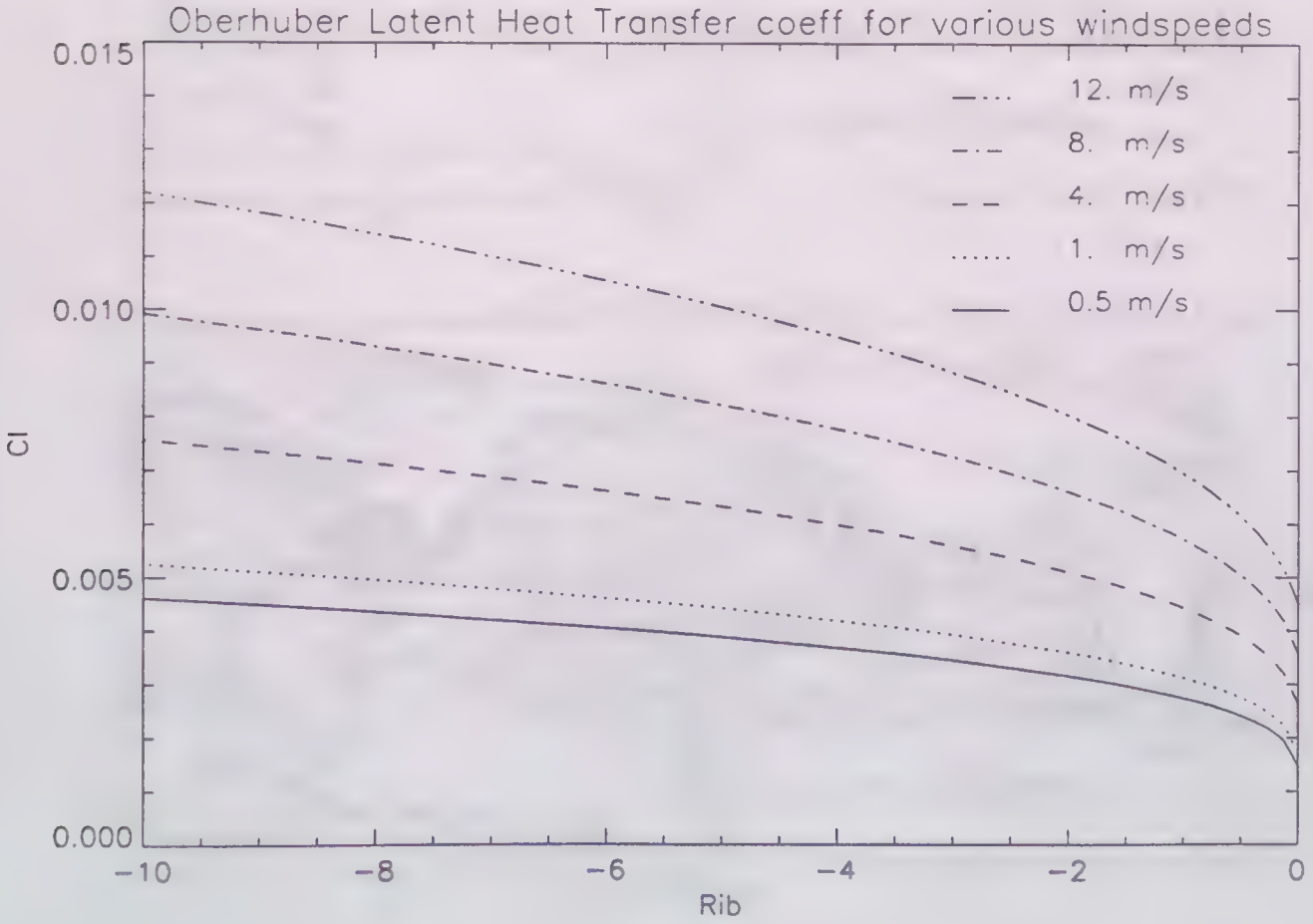
Oberhuber Latent Heat Transfer coeff for various windspeeds
0.015
0.010
0.005
0.000
CI
12. m/s
8. m/s
4. m/s
1. m/s
0.5 m/s
−10
−8
−6
−4
−2
0
Rib

Fig 11a

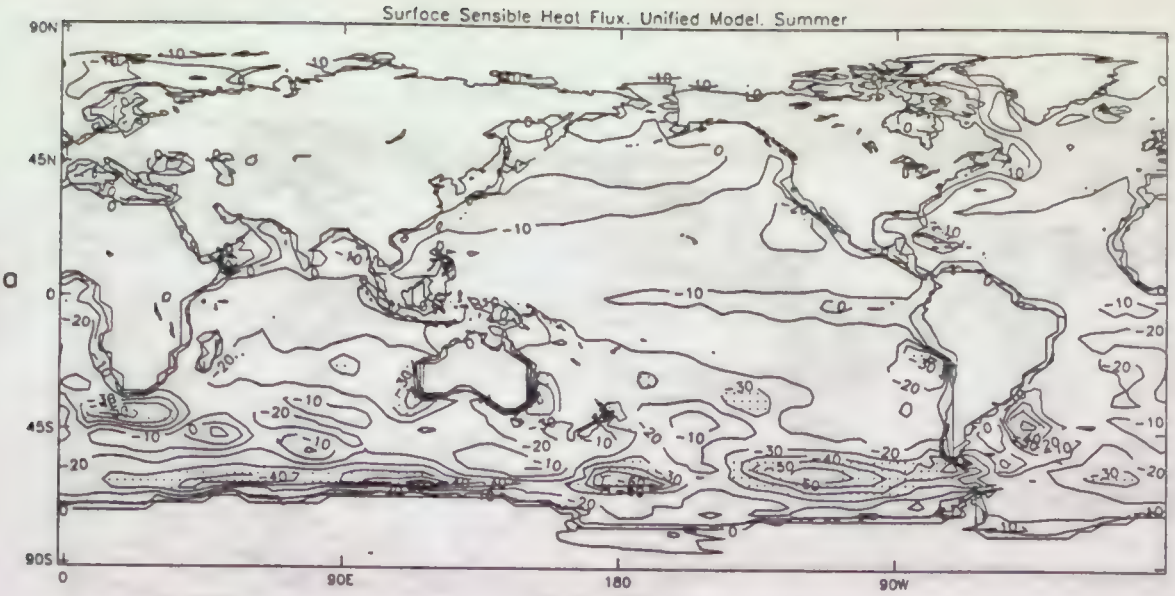

Fig 11b

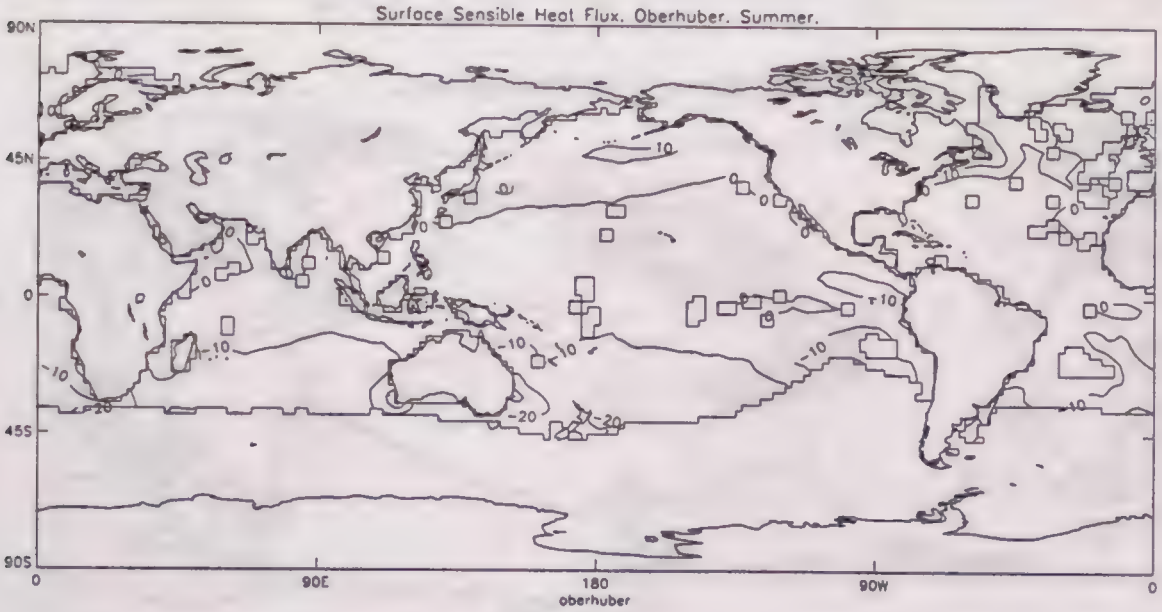

Fig 11c

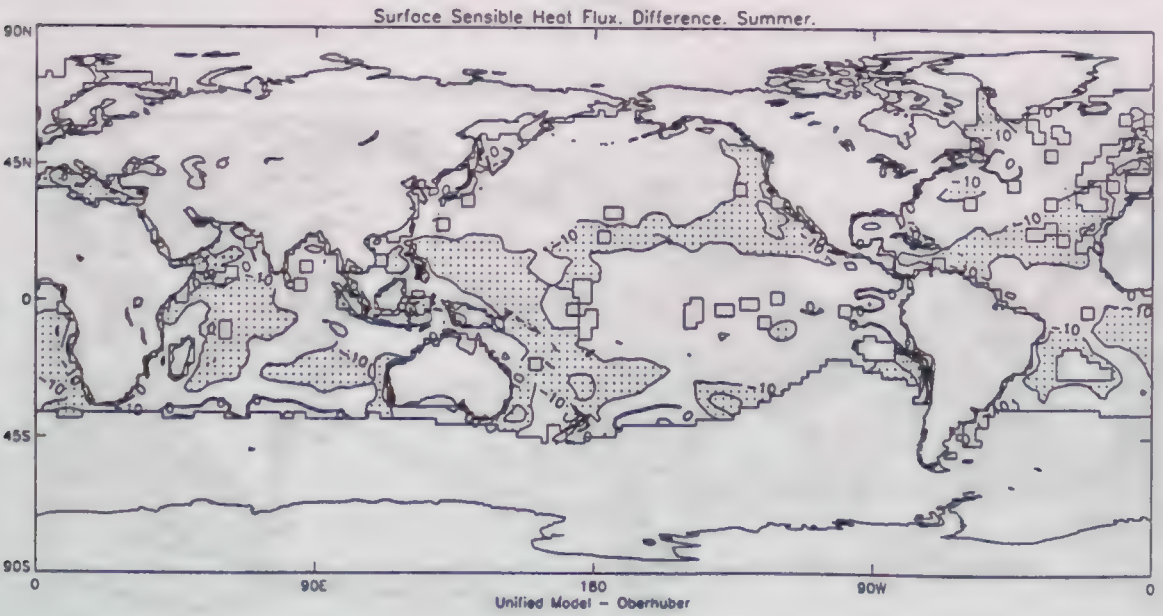

Fig 12a

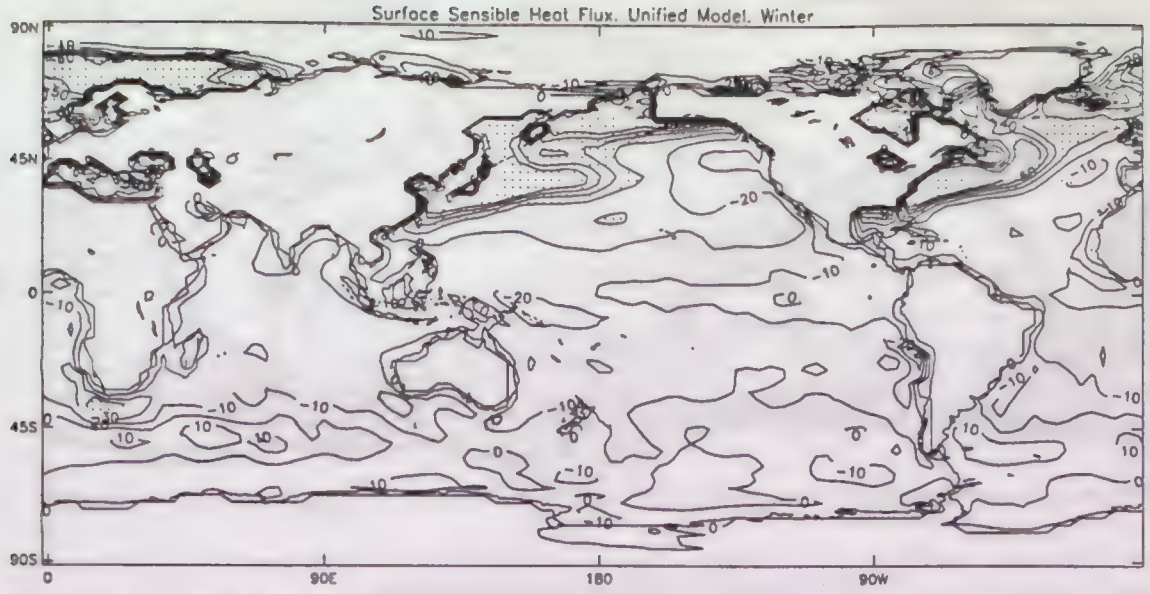

Fig 12b

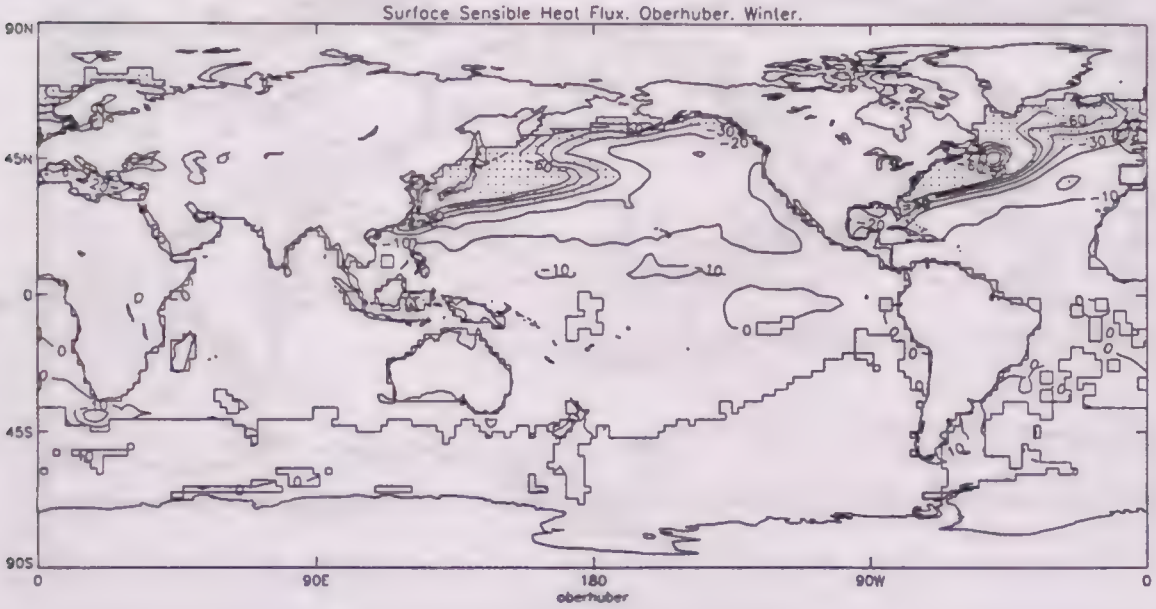

Fig 12c

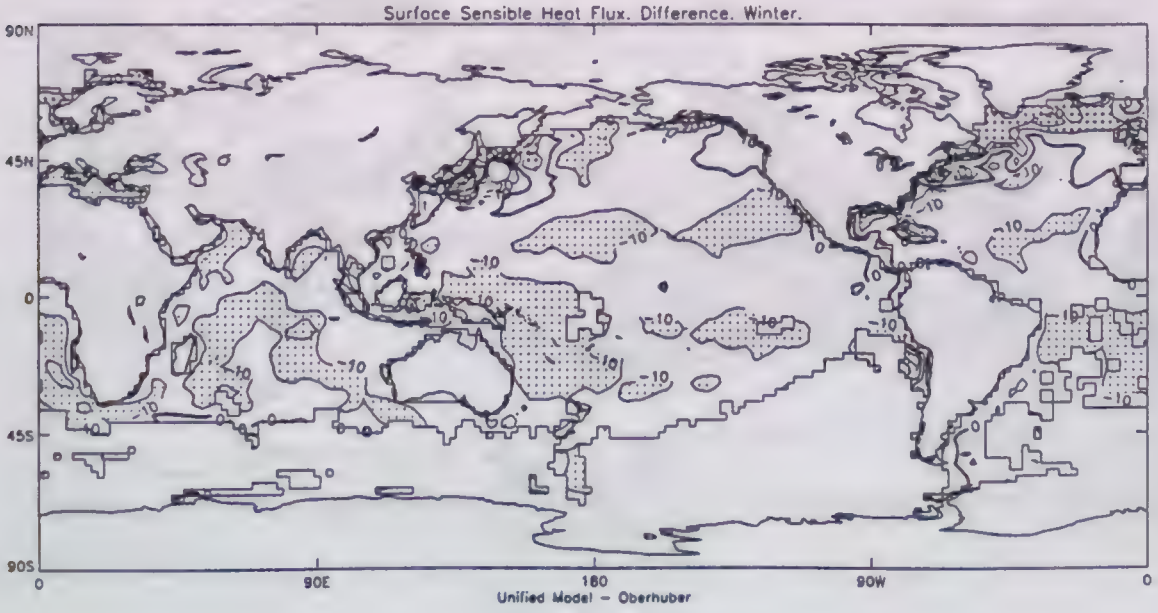

Fig 13a

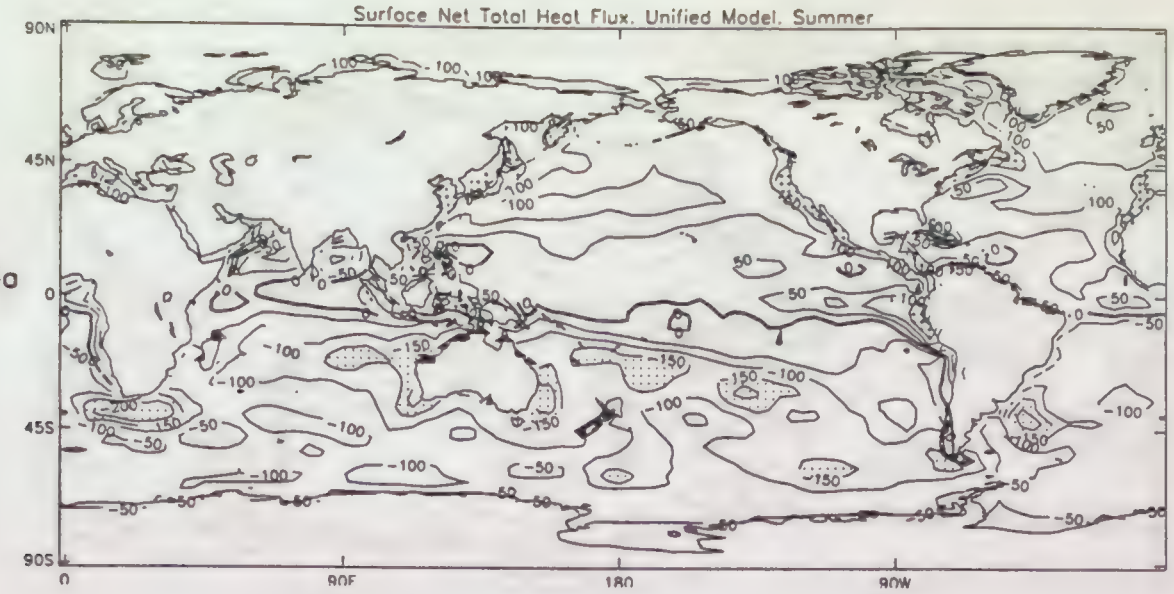

Fig 13b

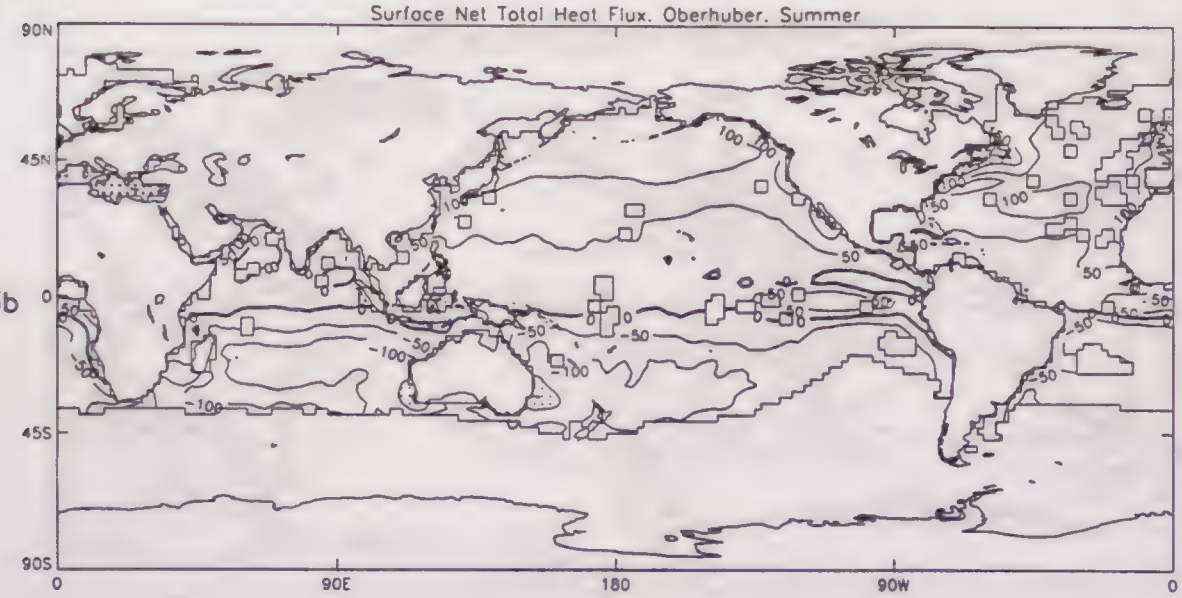

Fig 13c

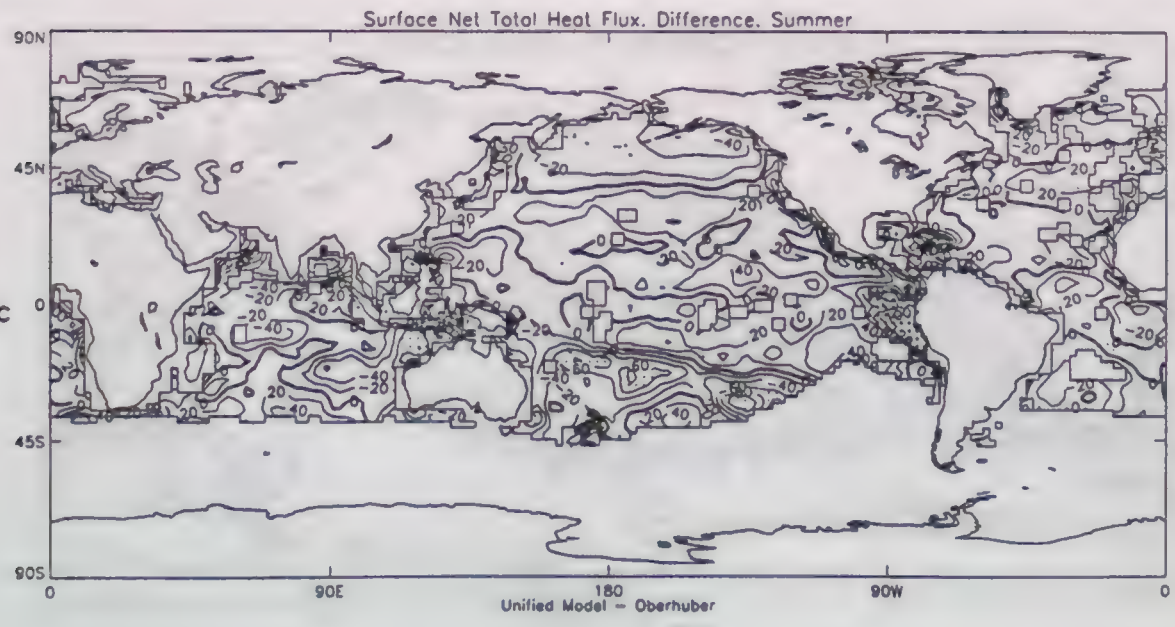

Fig 14a

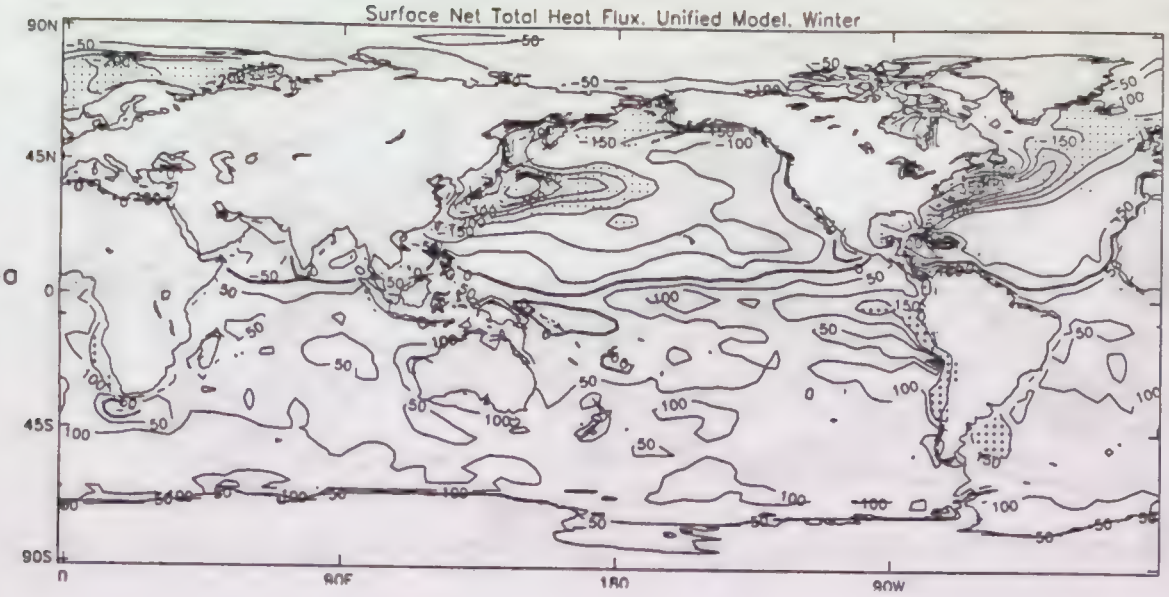

Fig 14b

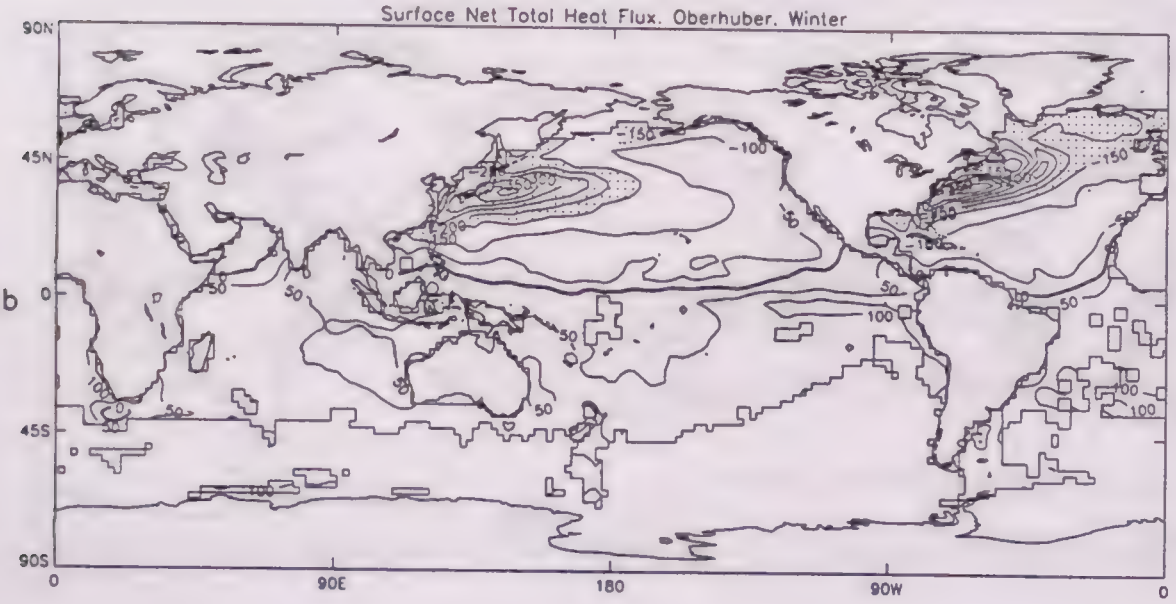

Fig 14c

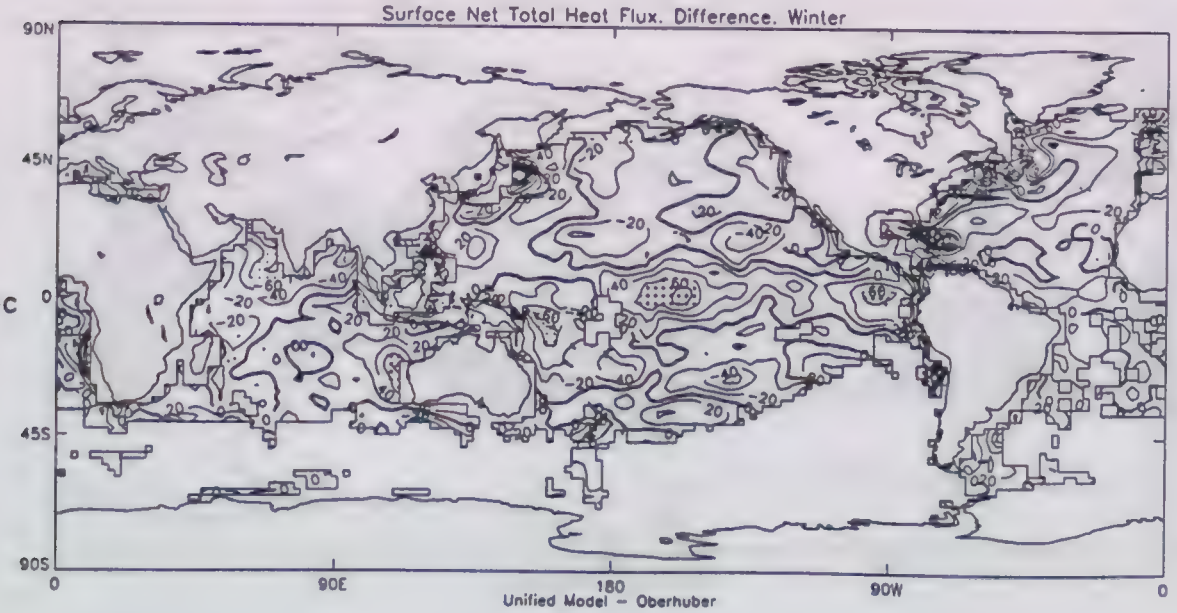

Fig 15a

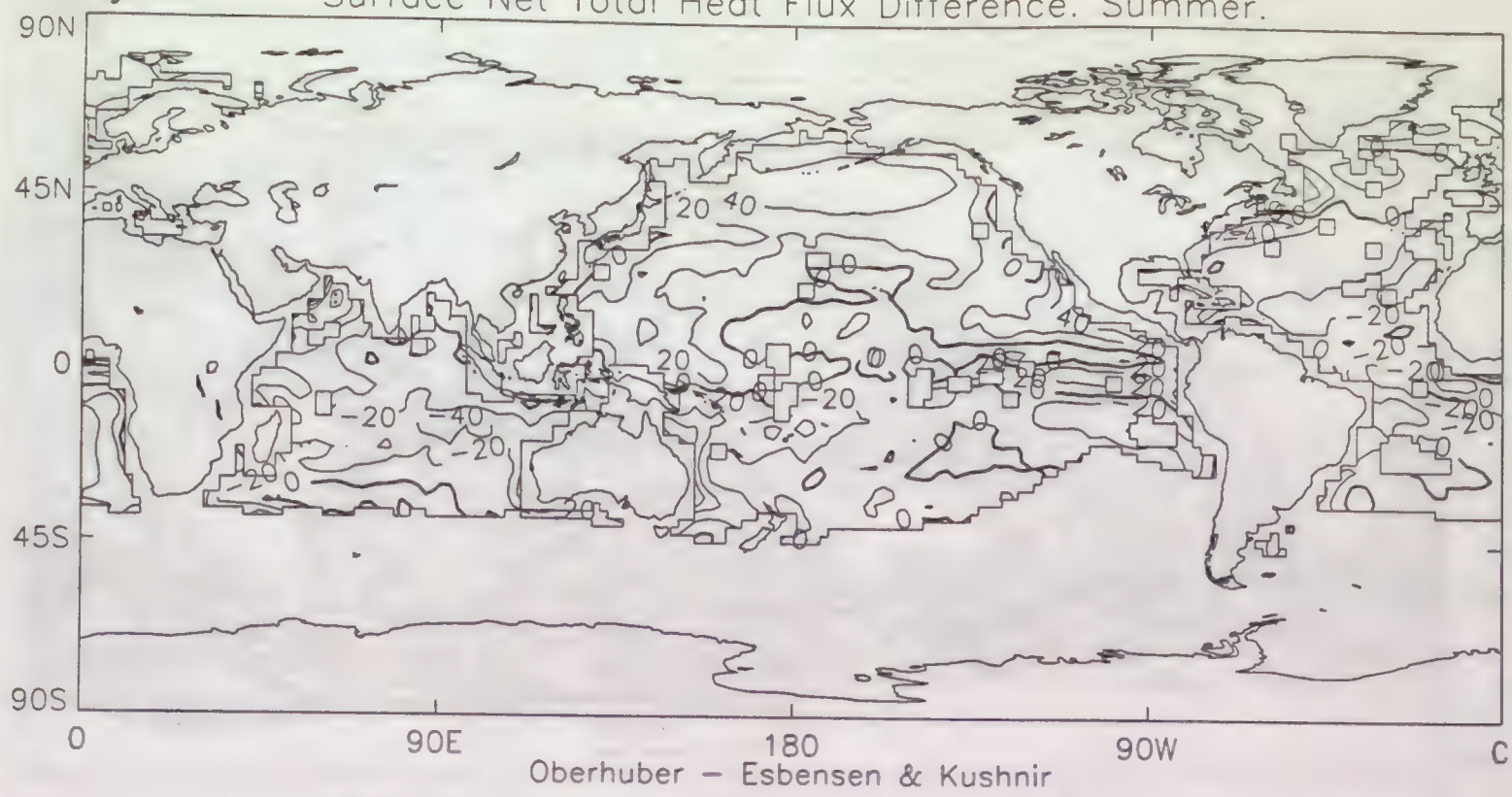

Fig 15b

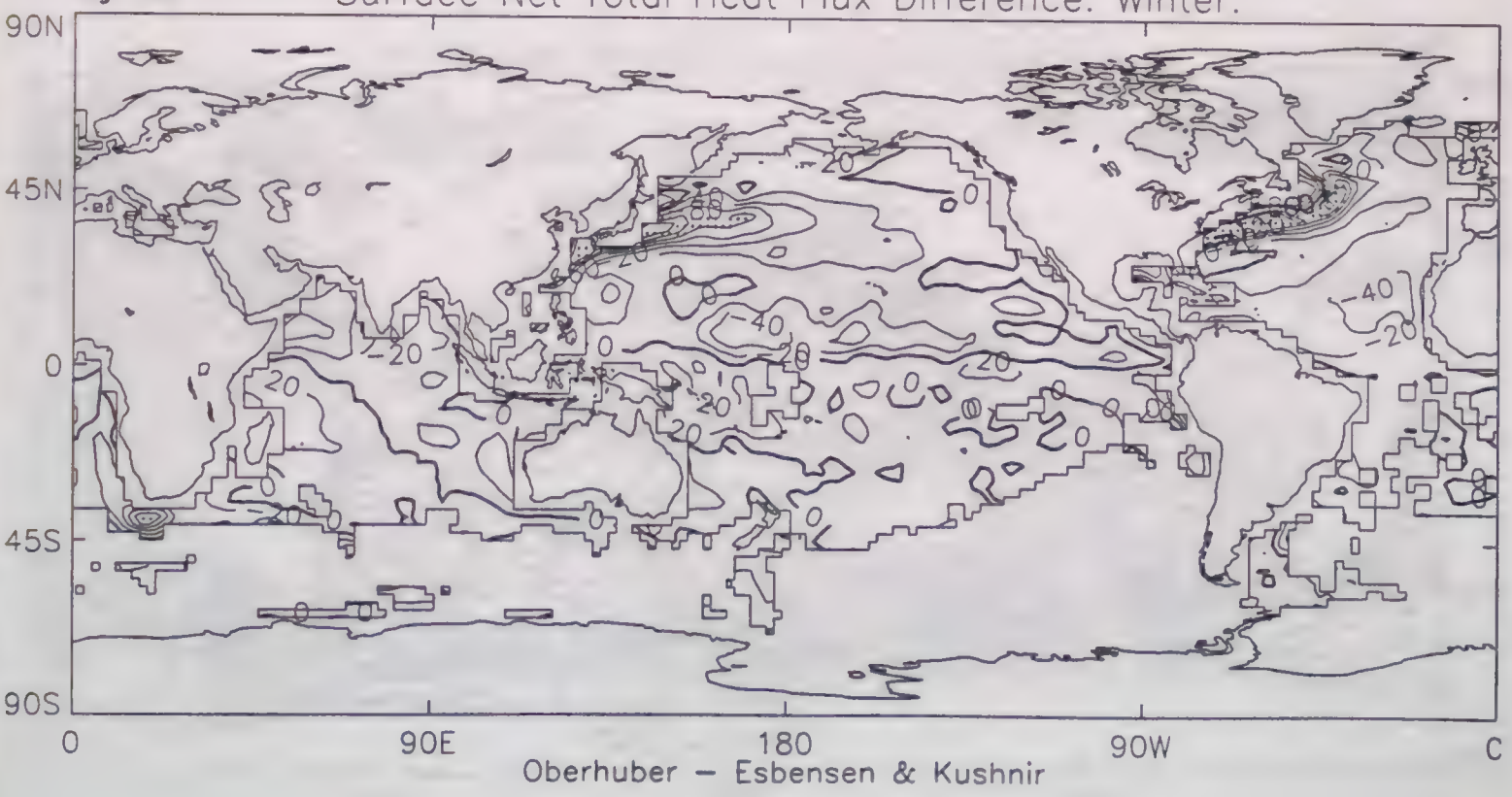

Fig 16a

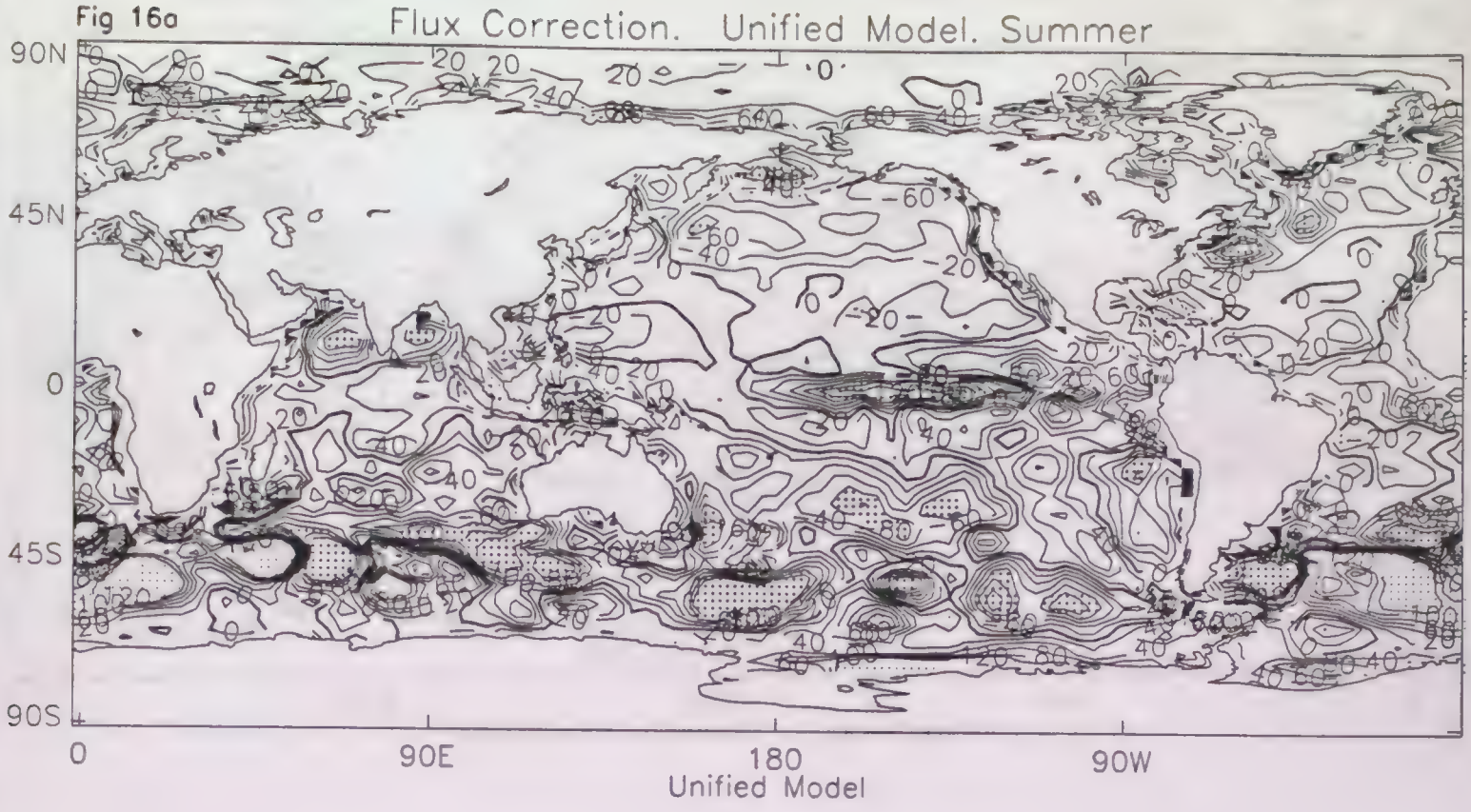

Fig 16b

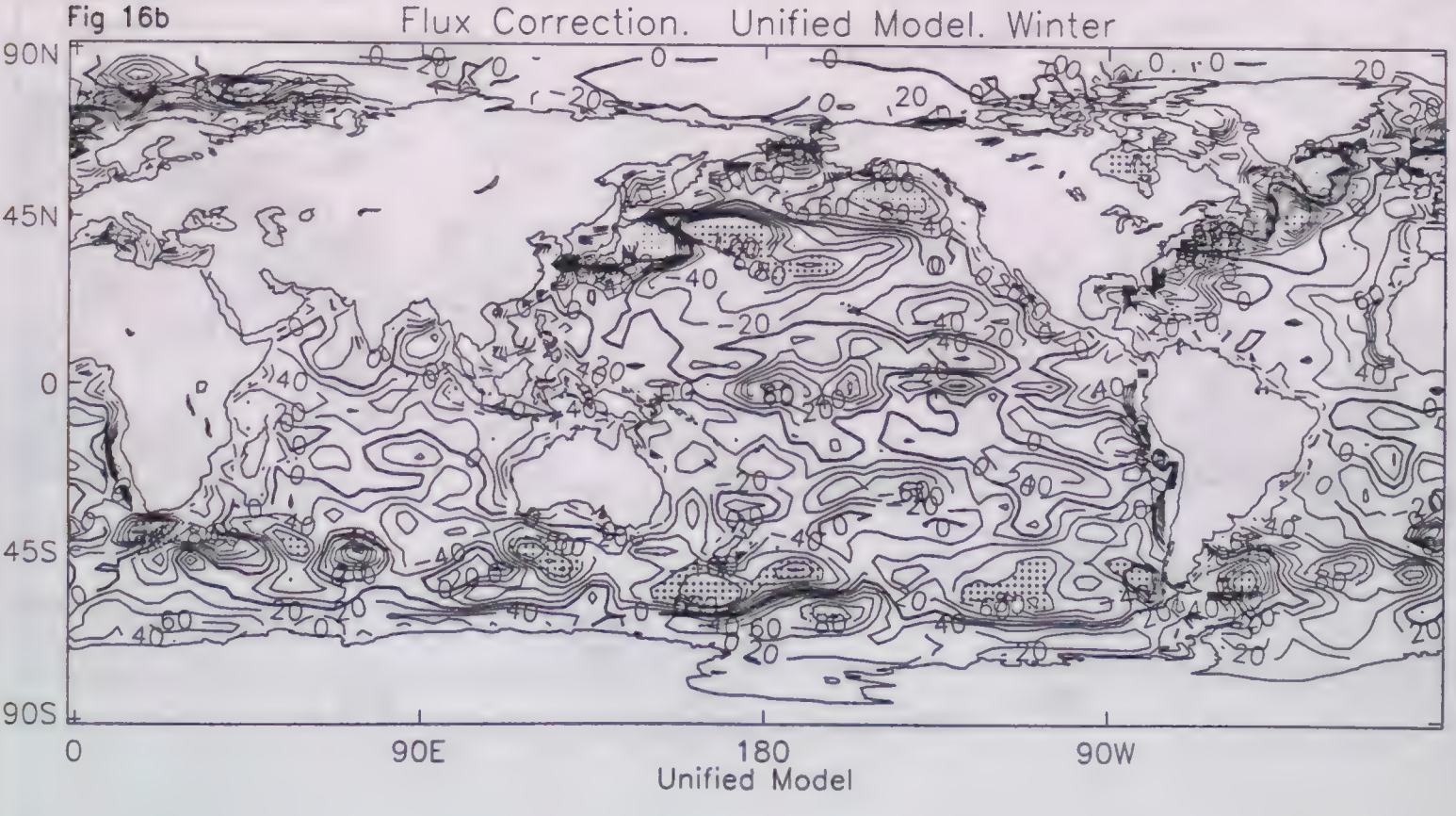

CLIMATE RESEARCH TECHNICAL NOTES

CRTN 1	Oct 1990	Estimates of the sensitivity of climate to vegetation changes using the Penman-Monteith equation. P R Rowntree
CRTN 2	Oct 1990	An ocean general circulation model of the Indian Ocean for hindcasting studies. D J Carrington
CRTN 3	Oct 1990	Simulation of the tropical diurnal cycle in a climate model. D P Rowell
CRTN 4	Oct 1990	Low frequency variability of the oceans. C K Folland, A Colman, D E Parker and A Bevan
CRTN 5	Dec 1990	A comparison of 11-level General Circulation Model Simulations with observations in the East Sahel. K Maskell
CRTN 6	Dec 1990	Climate Change Prediction. J F B Mitchell and Qing-cun Zeng
CRTN 7	Jan 1991	Deforestation of Amazonia - modelling the effects of albedo change. M F Mylne and P R Rowntree
CRTN 8	Jan 1991	The role of observations in climate prediction and research. D J Carson
CRTN 9	Mar 1991	The greenhouse effect and its likely consequences for climate change. D J Carson
CRTN 10	Apr 1991	Use of wind stresses from operational N.W.P. models to force an O.G.C.M. of the Indian Ocean. D J Carrington
CRTN 11	Jun 1991	A new daily Central England Temperature series, 1772-1991. D E Parker, T P Legg and C K Folland
CRTN 12	Jul 1991	Causes and predictability of Sahel rainfall variability. D P Rowell, C K Folland, K Maskell, J A Owen, M N Ward

CLIMATE RESEARCH TECHNICAL NOTES

CRTN 13	Jul 1991	Modelling changes in climate due to enhanced CO2, the role of atmospheric dynamics, cloud and moisture. C A Senior, J F B Mitchell, H Le Treut and Z-X Li
CRTN 14	Sep 1991	Sea temperature bucket models used to correct historical SST data in the Meteorological Office. C K Folland
CRTN 15	Aug 1991	Modelling climate change, and some potential effects on agriculture in the U.K. P R Rowntree, B A Callander and J Cochrane
CRTN 16	Aug 1991	The Boreal Forests and Climate G Thomas and P R Rowntree
CRTN 17	Aug 1991	Development of a Stratosphere-Troposphere Data Assimilation System. R Swinbank.
CRTN 18	Sep 1991	A study of asynchronous coupling using a simple climate model. M K Davey.
CRTN 19	Sep 1991	The Oceanic Carbon Cycle. N K Taylor
CRTN 20	Nov 1991	Worldwide ocean-atmosphere surface fields in Sahel wet and dry years using provisionally corrected surface wind data. M N Ward
CRTN 21	Dec 1991	Coupled tropical ocean global atmosphere models at the UKMO. M K Davey, C Gordon, S Ineson and S Lawrence
CRTN 22	Dec 1991	Empirical parameterisation of tropical ocean-atmosphere coupling. M Allen, M K Davey, D L T Anderson and P D Killworth
CRTN 23	Feb 1992	The temporal evolution of Equatorial Currents in the Indian Ocean D L T Anderson, D J Carrington, R A Corry and C Gordon
CRTN 24	Feb 1992	Stratospheric analyses provided by the U.K. Meteorological Office M J Bailey, A O'Neill and V D Pope

CLIMATE RESEARCH TECHNICAL NOTES

CRTN 25	Feb 1992	Modelling interannual variability in the Indian Ocean using momentum fluxes from the UKMO and ECMWF operational weather analyses. D L T Anderson and D J Carrington
CRTN 26	Mar 1992	A GCM simulation of the impact of Amazonian deforestation on climate using an improved canopy representation J Lean and P R Rowntree
CRTN 27	Mar 1992	The parameterization of rainfall interception in GCMs A J Dolman and D Gregory
CRTN 28	Jun 1992	Development of worldwide marine data eigenvectors since 1985 A W Colman
CRTN 29	Jun 1992	A tropical ocean model with reduced physics M K Davey
CRTN 30	Jun 1992	International Temperature Workshop, Boulder, Colorado, USA, 16 January 1992 Edited by D E Parker
CRTN 31	Jul 1992	Simulation of clear-sky outgoing longwave radiation over the oceans using operational analyses A Slingo and M J Webb
CRTN 32	Sep 1992	A prediction of the transient response of climate J M Murphy
CRTN 33	Nov 1992	LEPS scores for assessing climate model simulations and long-range forecasts. C K Folland
CRTN 34	Jan 1993	Stratospheric Data Assimilation System Guide Editer: R Swinbank
CRTN 35	Mar 1993	A Stratosphere-Troposphere Data Assimilation System R Swinbank and A O'Neill
CRTN 36	Mar 1993	Validation of hydrological schemes for climate models against catchment data. P R Rowntree and J Lean

CLIMATE RESEARCH TECHNICAL NOTES

CRTN 37	Apr 1993	Modelling of palaeoclimates: Examples from the recent past J F B Mitchell
CRTN 38	May 1993	A simulation of seasonality in ENSO forecast skill M K Davey, D L T Anderson and S Lawrence
CRTN 39	Jul 1993	ENSO Prediction experiments using a simple ocean-atmosphere model D-H Wu, D L T Anderson and M K Davey
CRTN 40	Sep 1993	Diagnosis of dynamic sea-surface and sea-level changes from the Cox ocean model J M Gregory
CRTN 41	Sep 1993	Seasonal variations of the clear-sky greenhouse effect: the role of changes in atmospheric temperatures and humidities M J Webb, A Slingo and G L Stephens
CRTN 42	Nov 1993	Sea-level changes under increasing atmospheric CO_2 in a transient coupled ocean-atmosphere GCM experiment. J M Gregory
CRTN 43	Dec 1993	Global and regional patterns of climate change: recent predictions for the Arctic P R Rowntree
CRTN 44	Feb 1994	The effect of changing horizontal diffusion in the atmospheric version of the unified climate model C D Hall and R A Stratton
CRTN 45	Mar 1994	Simulation of El-Niño/Southern Oscillation like variability in a global AOGCM and its response to CO_2 increase. S F B Tett
CRTN 46	Apr 1994	Global data required for monitoring climate change. D E Parker and C K Folland
CRTN 47	May 1994	Seasonal uptake of anthropogenic CO_2 in an ocean general circulation model. N K Taylor

CLIMATE RESEARCH TECHNICAL NOTES

CRTN 48	Jun 1994	A tropic-wide oscillation of boreal summer rainfall and patterns of sea-surface temperature. M N Ward, K Maskell, C K Folland, D P Rowell and R Washington
CRTN 49	Jun 1994	Simulation of the tropical Pacific using a simplified ocean model M A Balmaseda, D L T Anderson and M K Davey
CRTN 50	Sep 1994	Simulation of global mean temperature using a box-diffusion climate model P R Rowntree
CRTN 51	Sep 1994	Seasonal dependence of ENSO prediction skill M A Balmaseda, M K Davey and D L T Anderson
CRTN 52	Nov 1994	Simulation of the Indian Monsoon and Tropical Intraseasonal Variability by a General Circulation Model P M Inness and D Gregory
CRTN 53	Mar 1995	A comparison of modelled surface fluxes with climatological estimates. C Gordon and D K Wright